HHS Public Access

Author manuscript

Pain. Author manuscript; available in PMC 2024 January 01.

Published in final edited form as:

Pain. 2023 January 01; 164(1): 27–42. doi:10.1097/j.pain.0000000000002655.

Sympathetic modulation of tumor necrosis factor alpha-induced nociception in the presence of oral squamous cell carcinoma

Megan Atherton[1,2], **Stella Park**[3], **Nicole L. Horan**[2], **Samuel Nicholson**[3], **John C. Dolan**[3], **Brian L. Schmidt**[3], **Nicole N Scheff**[1,2,*]

[1]Department of Neurobiology, University of Pittsburgh, Pittsburgh PA USA

[2]Hillman Cancer Center, University of Pittsburgh Medical Center, Pittsburgh PA USA

[3]Bluestone Center for Clinical Research, DDS Program, College of Dentistry, New York University, New York, NY USA

1.0 Introduction

Head and neck squamous cell carcinoma (HNSCC) causes more severe pain and stress than other cancer[16; 38; 41; 82]. The oral cavity is densely innervated with both sensory[29; 55] and sympathetic[11] nerve fibers thought to mediate the cancer-induced pain and stress response. Sympathetic and sensory nerves can directly and indirectly communicate to mediate nociceptive signaling[89]. A better understanding of the biological mechanisms that couple sympathetic and sensory nervous system during tumorigenesis is needed.

Chronic stress can influence cancer progression via the sympathetic nervous system (SNS) [44; 75]. SNS fibers are activated during stress and release catecholamines, such as norepinephrine (NE), which act on adrenergic receptors to modulate cell behavior[20]. Oral tissues receive sympathetic innervation from the superior cervical ganglia (SCG) [33; 63]. Pathogical evaluation of nerves in HNSCC tumor tissue found that sympathetic nerve density was associated with lower survival rates[3]. Furthermore, plasma NE concentration was found to be nine times higher in HNSCC patients compared to patients with benign leukoplakia[8]. Preclinically, oral cancer was associated with increased sympathetic innervation in a rat model; sympathectomy resulted in smaller, less invasive cancers[65]. β-adrenergic receptors (β-AR) are present on tumor cells, and *in vitro* studies show that β-adrenergic signaling on tumor cells increased expression of vascular endothelial growth factor (VEGF), interleukins, and tumor necrosis factor alpha (TNFα) which are known to influence tumor progression[10; 48; 91; 92].

*Corresponding Author: Nicole Scheff, PhD, 5117 Centre Ave, Hillman Cancer Center Research Pavilion, Suite 1.19F, Pittsburgh, PA 15213, Phone: 412-623-7871.

Author contributions: All authors listed contributed substantially to the work. MA assisted in research design, conducted experiments, provided technical support, and edited the manuscript. SP, NH, and SN conducted animal behavior and molecular experiments, and performed data analyses. JD provided animal behavior expertise, technical support and edited the manuscript. BS assisted in research design and writing of the manuscript. NS designed the research, conducted experiments, performed data analyses, and wrote and edited the manuscript.

Conflict of Interest: Author John C. Dolan fabricates dolognawmeter assay devices for profit as the single-member limited liability company Gnatheon Scientific.

Cancer pain is associated with sensory and sympathetic nerve sprouting, as indicated in mouse models of cancer-induced bone metastasis[52] and pancreatic cancer[45]. Sensory neurons, which also express adrenergic receptors[24; 61], can be directly sensitized by NE during injury or inflammation[2; 5; 6; 13]. Baik and colleagues found that rats demonstrated intensified mechanical hyperalgesia in response to intradermal NE in the presence of inflammation in the L5 spinal nerve generated by complete Freud's adjuvant[5]. Clinically, sympathetic nerve blockade is a current therapeutic strategy to treat abdominal cancer-related pain[43]. There is also significant evidence that adrenergic antagonism improves cancer patient survival; prospective clinical trials that investigate the therapeutic value of beta blockers in visceral tumors are ongoing[42; 67]. However, patient reported pain and physiological symptom burden are not considered in these trials; the role of the SNS in oral cancer pain remains unknown.

We have previously demonstrated that TNFα is a prominent mediator in oral cancer-induced nociception using animal models[69; 74] and that TNFα concentration in oral cancer tissues correlates with reported pain scores in HSNCC patients[69]. In the current study, we explored the mechanisms of cancer-nerve interaction on the basis of the hypothesis that peripheral sympathetic signaling in the oral cancer microenvironment modulates cancer pain and tumor growth. We sought to (1) confirm the presence of sympathetic and sensory nerves innervating tumor tissue from HNSCC patients and a human xenograft mouse model, (2) determine the effect of sympathetic signaling via NE on oral cancer cell proliferation, tongue secretion of TNFα and trigeminal neuronal activity, and (3) determine the functional implications of systemic and local antagonism of sympathetic signaling on oral cancer-induced orofacial nociceptive behavior and tumor growth.

2.0 Materials and Methods

2.1 Patient data

We quantified sympathetic nerve presence in HNSCC patients who underwent surgical resection at the University of Pittsburgh Medical Center between 2015 and 2018. Thirteen patients were collected for these analyses; all were >18 years, underwent surgical resection for squamous cell carcinoma of the oral cavity or oropharynx, and had perineural invation (PNI) denoted in the pathology report by a oral and maxillofacial pathologist. Patients with recurrent disease or second primaries were excluded. Demographics and clinical characteristics were obtained from medical record review and included: age at diagnosis, sex, race, surgical procedure [i.e., oropharyngectomy (tonsil, base of tongue), mandibulectomy/composite resection, glossectomy/floor of mouth resection, laryngectomy/pharyngectomy], tumor size, nodal status, HPV status for oropharyngeal tumors, history of tobacco use, history of alcohol use, PNI (yes/no) and extracapsular spread (yes/no/not evaluated) (Suppl Table 1). HNSCC tissue from patients was acquired through the University of Pittsburgh Medical Center (UPMC) Hillman Cancer Center's Head and Neck SPORE (P50CA097190; R.L. Ferris, PI) collection of head and neck cancer tissue specimens. All patients provided informed written consent; this study was approved by the Institutional Review Board associated with University of Pittsburgh Cancer Institute (STUDY20050058).

2.1 Animals

Adult (10-12 weeks, 20-25 g) male and female C57BL/6 (stock #000664; Jackson Labs, Bar Harbor, ME) and athymic nude (stock #002019, Jackson Labs) mice were used for *in vitro* experiments. Adult female athymic nude mice were used for *in vivo* experiments. All mice were housed in a temperature-controlled room on a 12:12-hour light cycle (0700-1900 hours light), with unrestricted access to food and water. Researchers were trained under the Animal Welfare Assurance Program. All procedures were approved by the New York University and University of Pittsburgh Institutional Animal Care and Use Committees and performed in accordance with National Institutes of Health guidelines for the use of laboratory animals in research.

2.2 Xenograft oral cancer pain model

Mice were inoculated with $1x10^5$ HSC-3 cells in 30 μL of 1:1 Dulbecco's modified Eagle's medium (DMEM, Gibco, Waltham, MA) and Matrigel (Corning, Corning, NY) into the anterior lateral portion of the tongue as previously described[95]. Nociceptive behavior was measured twice per week using a dolognawmeter assay for the duration of the experiment. To inhibit β-adrenergic signaling systemically, propranolol (0.25 g/L) was administered in the drinking water, as previously done[30; 79] to avoid unnecessary stress in tumor-bearing mice, starting at post inoculation day (PID) 5. The propranolol group consumed, on average, 17.17±1.8 mL of water per day per mouse. Based on these calculations, tumor-bearing mice that received propranolol ingested on average 0.859±0.09mg per day per mouse; thus, on average about 0.214mg reached circulation following first pass metabolism. This dose is consistent with previous publications in which propranolol doses were given via daily intraperitoneal (i.p.) administration[15; 60]. To induce a chemical sympathectomy, guanethidine monosulfate (GTD, 50 mg/kg) was injected i.p. 2x per week starting at PID 7. This was continued throughout the protocol, based on the drug's pharmacokinetic properties, half-life (~1.5 days), and previous reports[80]. For both studies, body weight was recorded once per week. Tongue tumor size was quantified at PID 28 after GTD treatment. At PID 28, tongues were harvested, fixed in 10% neutral buffered formalin, bisected, paraffin-embedded with cut side down, and sectioned at 5μm thickness through the entire block (about 50 sections). Average tumor area relative to total tongue area in the 1^{st}, 10^{th}, 20^{th}, 30^{th} and 40^{th} section was quantified using hematoxylin and eosin (H&E) stain and ImageJ (NIH, Bethesda, MD). The experimenters conducting the behavioral tests (SP) and tumor quantification (SP, SN) were blinded to the treatment groups.

2.3 Immunohistochemistry

2.3.1. Head and neck cancer tumor tissue staining: Developmental Pathology Laboratory shared resource in the Department of Pathology obtained the paraffin-embedded tissue blocks and performed the sectioning (5μm) and staining. Serial sections were stained with either mouse monoclonal anti-S100 (1:100, abcam cat# ab4066), rabbit anti-tyrosine hydroxylase (TH) (1:500, Millipore Sigma Cat#AB152), or rabbit anti-TRPV1 (1:600, Thermo Scientific). Immunoreactions were visualized with diaminobenzidine (DAB) horseradish peroxidase (HRP) substrate and counterstained with hematoxylin. The sections were scanned at 10x, 20x, and 40x magnification and S100 labeling was used to identify

all nerve bundles. Total S100 immunoreactive area was quantified using Aperio ImageScope software (Leica Biosystems). Within each nerve bundle, TH and TRPV1 immunoreactive area was quantified, summed for total TH or TRPV1 area and the percent of TH+ or TRPV1+ area relative to total S100 area was then calculated.

2.3.2. Mouse tongue tissue staining

Optical clearing: Athymic nude mice (2 naïve and 4 HSC-3 tumor-bearing mice) under 3-5% isoflurane anesthesia were transcardially perfused with phosphate buffered saline (PBS) followed by 4% paraformaldehyde solution (PFA). Tongues were bisected along sagittal plane and stored in 4% PFA at 4°C until needed. Optical clearing was achieved using the established PEGASOS protocol[35]. For antibody staining, tongue tissue was incubated in blocking solution containing 3% goat serum and 1% triton X-100 overnight. The tissue was then incubated in primary antibody rabbit anti-TH (1:250, Millipore Sigma) at 4°C for 3 days followed by secondary antibody Alexa goat anti-rabbit 647 (1:250, Thermo Fisher) at 4°C for 48 hours. Tissue was imaged by the Center for Biologic Imaging (CBI) at University of Pittsburgh using a Caliber Ribbon Scanning Confocal S228.

Immunohistochemistry: Tumor tongue tissue was dissected, postfixed for 24 hours in 4% PFA, and cryoprotected in 30% sucrose at 4°C overnight. Tongue tissue was then embedded in Tissue-Tek OCT compound (Sakura Finetek, Torrance, CA), sectioned (20μm) coronally starting at the tip, and mounted on Superfrost Plus slides (Fisher Scientific). Slides were incubated in one of the following primary antibodies: rabbit anti-PGP9.5 (1:250, BosterBio), rabbit anti-TH (1:500, Millipore Sigma), or rabbit anti-CGRP (1:500, Cell Signaling) in PBS containing 1% bovine serum albumin overnight at room temperature. Slides were extensively washed in PBS, incubated in goat anti-rabbit Alexa fluor 594 (1:250, Jackson ImmunoResearch) for 2.5 hours and extensively washed. To quench autofluorescence due to collagen and striated tongue muscle, TrueVIEW autofluorescence quenching kit with DAPI (Vector Laboratories, Newark, CA) was used according to manufactuerer's instructions.

2.3.3. Mouse sensory and cervical ganglia staining—

At least 10 days prior to tissue harvest, the retrograde tracer 1,10-dioctadecyl-3,3,30,30-tetramethy lindocarbocyanine perchlorate (DiI, Invitrogen, Carlsbad, CA, USA) was injected peripherally into the anterior lateral tongue to retrograde label tongue afferents in 6 adult C57Bl/5 and 6 adult athymic nude mice. The tracer was dissolved at 170 mg/mL in DMSO, diluted 1:10 in 0.9% sterile saline, and injected bilaterally using a 30 g needle for a total volume of 5-7μL per tongue. Mice under 3-5% isoflurane anesthesia were transcardially perfused with PBS followed by 4% PFA. The trigeminal ganglia (TG) and superior cervial ganglia (SCG) were dissected, postfixed for 1 hour in 4% PFA, and cryoprotected in 30% sucrose at 4°C overnight. TG and SCG were embedded in Tissue-Tek OCT compound (Sakura Finetek, Torrance, CA), sectioned (14μm), and mounted on Superfrost Plus slides (Fisher Scientific). Slides were incubated in primary antibody rabbit anti-TH (1:500, Millipore Sigma) in PBS containing 1% bovine serum albumin overnight at room temperature. Slides were extensively washed in PBS, incubated in goat anti-rabbit Alexa fluor 488 (1:250, Jackson ImmunoResearch) for 2.5 hours, extensively washed, and cover-slipped with Fluoro-Gel II mounting media containing DAPI

(Electron Microscopy Sciences). Using a Leica DMi8 microscope with LAS software, TG sections were photographed at 20x magnification within the intersection of the mandibular and maxillary branch, where most retrograde labeled trigeminal tongue neurons reside. Trigeminal ganglia neurons (TGN) with distinct nuclei and at least 50% of the cell area labeled with DiI were counted in every fifth section (9 sections/mouse; 3 males, 3 females per genotype). ImageJ software (NIH, Bethesda, MD) was used to count retrograde labeled neurons which overlapped with anti-TH immunoreactivity per animal.

2.3.4. Human cancer cell line staining—Human cancer and non-tumorigenic cells were plated in a Lab-Tek II 4-well chamber slide and allowed to proliferate for 24-48 hours to reach 70-80% confluency. Cells were then treated with either cell culture media alone or cell culture media containing vehicle (0.03% HCl), 1μM NE, 10μM NE or 1μM salbutamol. Adrenergic β2 competitive agonist (1μM ICI 118,551) was added 1 hour prior to addition of the NE. After 24hrs, cells were washed with PBS and fixed in 4% PFA for 30min at 4°C. Following fixation, the chamber insert was removed, and the slides were washed extensively. They were then incubated in blocking buffer containing 1% albumin bovine serum (BSA) and 22.57mg/ml glycine for 30min followed by rabbit anti-β-AR2 conjugated to FITC (1:500, Alomone, Jerusalem) diluted in PBS containing 1% BSA at 4°C overnight. Finally, the slides were washed in PBS and cover-slipped with Fluoro-Gel II mounting media containing DAPI. Cells were photographed at 20x magnification using LAS software and a Leica DMi8 microscope with the gain set to 1. Vehicle-treated cells were used to threshold signal for quantification and settings were maintained across treatment groups. Cells with distinct nuclei were counted in 3 slides (5 regions per slide: upper right quadrant, upper left quadrant, middle, lower right quadrant, lower left quadrant) within each treatment group. ImageJ software (NIH, Bethesda, MD) was used to count cells with distinct nuclei that overlapped with anti-β-AR2 immunoreactivity.

2.4 Cell culture and supernatant collection

All cell lines were cultured in 10 cm diameter cell culture dishes at 37°C with 5% CO_2. Oral squamous cell carcinoma (SCC) cell lines HSC-3 (Sekisui XenoTech, Kansas City, KS) and and non-tumorigeneic cell line HaCaT were cultured in DMEM supplemented with 10% fetal bovine serum (FBS) and penicillin/streptomycin (P/S, 50 U/mL). SCC cell line SCC-4 (ATCC, Manassas, VA) was cultured in DMEM/F12 (Gibco, Waltham, MA) supplemented with 10% FBS and P/S. Dysplasic oral keratinocyte cell line DOK (Sigma Aldrich, St. Louis, MO) was cultured in DMEM supplemented with 10% FBS, P/S, and 5μg/mL hydrocortisone. For collection of supernatant (SN), the culture medium was changed to serum-free DMEM without phenol red (3 mL total volume) when cells reached 70-80% confluency (1.5 x 10^6 cells). Cells were then incubated for an additional 48 hours. Following incubation, cell culture SN was collected, centrifuged at 300xg to remove cell debris, and frozen at −20°C until needed. SN from cell lines HSC-3 and SCC-4 was collected from passages 3 and 12 respectively. SN from DOK was collected from passage 7.

2.5 qPCR

Total RNA was isolated from pelleted cells (1-1.5x10^6) from cell lines and whole TG using the Qiagen RNeasy Plus Mini Kit (Qiagen Inc.). Reverse transcription was performed

with Quantitect Reverse Transcription Kit (Qiagen Inc.) according to the manufacturer's instructions. cDNA was diluted with nuclease free water to a 5 ng/μL concentration. For single cell analysis, DiI-positive single neurons were identified using fluorescence microscopy, picked up using glass capillaries (World Precision Instruments) held by micromanipulator (Sutter Instruments), headstage (EPC10 HEKA) and electrode holder under brightfield optics. Cell size was not considered during selection. Each cell was transfered into a 0.2 ml PCR tube containing 9μl of single cell lysis solution and Dnase I from Single Cell-to-CT™ Kit (Thermo Fisher Scientific), incubated for 5 minutes and immediately stored at −80°C until further use. Cells were collected within 1 h of removal from the incubator and within 8 h of removal from the animals (n=2 C57Bl/6 mice). Reverse transcription, cDNA pre-amplification and Real-Time PCR were executed per manufacturer's instructions. Relative expression levels of adrenergic receptors were assessed using TaqMan Gene Expression Assays and TaqMan Gene Expression Master Mix (Thermo Fisher Scientific), using a 96 well Quantstudio 3 Real-Time PCR System (Thermo Fisher Scientific). We used assays from Life Technologies for the following genes: *ADRB1* (Hs02330048_s1), *ADRB2* (Hs00240532_s1), *ADRB3* (Hs00609046_m1), *Adra1a* (Mm00442668_m1), *Adra1b* (Mm00431685_m1), *Adra1d* (Mm01328600_m1), *Adra2a* (Mm07295458_s1), *Adra2b* (Mm00477390_s1), *Adra2c* (Mm00431686_s1), *Adrb1* (Mm00431791_s1), *Adrb2* (Mm02524224_s1), *Adrb3* (Mm02601819_g1). The housekeeping genes *ACTB* (Hs01060665_g1) and *Gapdh* (Mm99999915_g1) were used as the internal control gene for human and mouse respectively. Relative quantification analysis of gene expression data was calculated using the $2^{-\Delta Ct}$ method. For single cell PCR, any cell with a *Gapdh* Ct threshold of 27 or higher was excluded from further analysis. Genes were considered 'not expressed' if one sample either failed to detect expression or the Ct was above 38.

2.6 Proliferation assay

To quantify the effect of adrenergic signaling on cancer cell proliferation, 1000 cells (HSC-3, SCC-4, DOK) were seeded in individual wells in a 96 well plate containing media supplemented with 10% FBS. After 4 hours, media was replaced with serum-free media for 24 hours to drive cell cycle synchronization. To conduct a quantitative MTS colorimetric proliferation assay, control wells received vehicle (0.03% HCl and EtOH or 0.03% water), and experimental wells received varying doses of NE (0.1 - 10μM, 20mM stock in HCl), 10μM NE plus 10μM propranolol (20mM stock in EtOH) or varying doses of salbutamol (0.1 - 1μM, 10mM stock in water) or 1μM salbutamol plus 10μM propranolol in a total volume of 100μl. After 24 hours, 20μL of MTS (Promega BioSciences) was added to each well. Plates were incubated at 37°C for 1 hour. The samples were then quantified at 490 nm using GloMax-Multi Microplate Multimode Reader (Promega). The samples on each plate were run on three different cell line passages, and the experiment was repeated in triplicate.

2.7 Enzyme-linked immunosorbent assay (ELISA)

TNFα protein concentration was measured in cell line SN and homogenized tongue tumor tissue by ELISA (Sigma Aldrich Cat# RAB1089-1KT). Cells were seeded into a 6-well plate at $2x10^5$ cells per well and allowed to come to 70-80% confluency. Cells were then treated with one of 6 treatments in 600μl of serum free colorless DMEM: 10μM

NE, 10μM NE + 10μM propranolol, 10μM NE + 10μM ICI 118,551, 1μM salbutamol, 1μM salbutamol + 10μM propranolol. Receptor antagonists (e.g. propranolol, ICI 118,551) were added 1 hour prior to addition of the agonist (e.g. NE, salbutamol). After 48 hours cell culture, SN was collected, treated with 6μl HALT Protease Inhibitor Cocktail (Pierce, Rockford, IL) and stored at −80°C until needed. For mouse tumor tissue, mice were perfused with PBS and tongues were harvested and snap frozen in dry ice. Tumor tissue was then dissected and minced on dry ice and stored at −80°C until needed. Frozen minced tissue (20–40 mg) was homogenized in 500μl RIPA buffer (Pierce Biotechnology) containing 5μl HALT Protease Inhibitor Cocktail and agitated for an additional 15min at 4C. Lysates were centrifuged at 16,000 rpm for 15 min. Supernatants were removed and used immediately. Total protein concentrations were determined for all samples using a Bradford Assay (Bio-Rad Laboratories, Inc.) and ELISA was run per the manufacturer's instructions. The optical densities of the standards and samples were read at 450 nm using a GloMax Explorer GM3500 Microplate Reader (Promega). TNFα protein concentrations were calculated based on manufacturer's instructions and normalized to total protein in the sample.

2.8 TGN primary culture

Adult C57BL/6 mice under 3-5% isoflurane anesthesia were transcardially perfused with cold Ca^{2+}/Mg^{2+}-free Hank's balanced salt solution (HBSS, Invitrogen). Bilateral TG were dissected into cold HBSS and dissociated as previously described[74]. Cells were plated in DMEM/F12 containing 10% FBS and P/S. Coverslips were flooded 2 hours later with DMEM/F12 containing 10% FBS and antibiotics, then stored at 37°C. Experiments were performed within 8 hours of tissue harvest.

2.9 Calcium imaging

Dissociated TGN were incubated with 5 μM Ca^{2+} indicator Fura-2AM (Invitrogen, Carlsbad, CA, USA) at room temperature for 30 min in DMEM without phenol red (colorless). Coverslips were placed in a recording chamber and continuously infused with colorless DMEM at room temperature. Imaging was done at 20X magnification in fields containing ≥ 5 neurons and at least 2 coverslips were tested per mouse. To measure the neuronal response to NE, 10μM NE in normal bath (130mM NaCl, 3mM KCl, 2.5mM $CaCl_2$, 0.6mM $MgCl_2$, 10mM HEPES, and 10mM Glucose) was applied to the cells for 30s. 10μM NE was chosen as the most relevant concentration as that is what was previously published as being physiologically relevant in the tumor microenvironment of cancer patients[85]. To measure the neuronal response to the cancer cell line SN and SN from cancer cells treated with 10μM NE, SN was applied for 30 sec followed by a 30 sec wash with colorless DMEM. TNFα–TNFR interaction modulator C87 (5 mM stock in dimethylsufoxide [DMSO]; EMD Millipore, Billerica, MA) was used to inhibit TNFα signaling in the presence of oral cancer SN treated with NE. C87 (1μM) was added into the normal bath perfusion and cells were exposed to C87 for 1 min to ensure the drug did not elicit a Ca^{2+} response followed by oral cancer SN treated with NE supplemented with C87 (1μM). C87 was added to the supernatant 15-30min prior to application onto neurons and incubated at room temperature. The vehicle control for C87 (0.02% DMSO) was absent in the supernatant samples for these studies. To test for cell viability, 30 mM KCl in colorless DMEM was applied for 4 sec at the end of each experiment. Cancer cell SN and KCl were

applied with a fast-step perfusion system (switching time <20 ms; Warner Instrument Co, Model SF-77B). A change in intracellular Ca^{2+} concentration ($[Ca^{2+}]_i$) ≥ 20% of baseline was considered as a response to stimulus. The magnitude of the response was calculated as (Peak $[Ca^{2+}]_i$) – (Baseline $[Ca^{2+}]_i$). Fluorescence data was acquired by a Nikon Eclipse Ti microscope at 340 nm and 380 nm excitation wavelengths and analyzed with the TI Element Software (Nikon, Melville, NY, USA). $[Ca^{2+}]_i$ was determined from Fura-2AM ratio. Calibration of imaging software to convert Fura-2 ratio following *in situ* calibration experiments was performed as previously described[26; 73].

2.10 Dolognawmeter orofacial pain behavior assay

The dolognawmeter assay and automated device quantifies gnawing activity. The outcome variable (gnaw-time) is the time required by a rodent to gnaw through the second of two obstructing polymer dowels in series (a discrete gnawing task) that block escape of a rodent confined in a narrow tube. Extended gnaw-time relative to baseline values is a validated index of orofacial nociception in mice with oral cancer[23]. Each mouse is placed into a confinement tube, where forward movement of the rodent in the tube is obstructed by 2 polymer dowels. The mouse voluntarily gnaws through both dowels to escape the device. The second of two sequentially obstructing polymer dowels is connected to a digital timer. The timer automatically records the duration required for the mouse to sever the second dowel. To acclimatize the mice and improve consistency in gnawing behavior, all mice were trained for 7-9 sessions in the dolognawmeter. Training was accomplished by placing the mice in the device and allowing them to gnaw through the obstructing dowels in the same manner as the subsequent experimental gnawing trials. For the xenograft oral cancer pain model, a baseline gnaw-time (mean of the final 3 training sessions) was established for each mouse followed by behavioral testing twice per week for up to 5 weeks. The investigator was blinded to the treatment groups. Each mouse was compared to its own baseline gnaw-time, and data are presented as a percent change ± standard error of the mean.

2.11 Drugs:

In *in vivo* studies, propranolol (0.25 g/L in water, Sigma-Aldrich; vehicle control = water) and guanethidine monosulfate (GTD, 50 mg/kg in saline, Cayman Chemical Company; vehicle control = 50μl saline) were administered to determine the effect of sympathetic signaling on orofacial nociceptive behavior and tumor growth. In *in vitro* studies, drugs and controls were added to cell culture media. (−)-norepinephrine (1-10μM. 20mM stock in 1N HCl, Sigma Aldrich; vehicle control = 0.05% HCl) and salbutamol hemisulfate (0.1-1μM, 10mM stock in water Fisher Scientific; vehicle control = 0.01% water) were used to drive cell proliferation, β2-ADR expression, and TNFα secretion in cell lines. Adrenergic reception inhibition was achieved using ICI 118,551 hydrochloride (1μM, 10mM stock in water, Medchem Express; vehicle control = 0.01% water) and (+/−)-propranolol hydrochloride (10μM, 20mM stock in ethanol, Sigma-Aldrich; vehicle control = 0.05% EtOH). TNFα–TNFR interaction modulator C87 (1μM, 5 mM stock in dimethylsufoxide [DMSO]; EMD Millipore) was used to inhibit TNFα signaling in Ca^{2+} imaging studies.

2.12 Statistical Analysis:

Statistical significance was set at $p < 0.05$. All statistical analyses were performed using Prism (version 8) statistical software (Graphpad Software Inc., La Jolla, CA, USA). Results were presented as mean ± standard error of the mean. Box/scatter or violin/scatter configurations were used to show the biological variability. *In vivo* mouse model experiments were set as a 2x2 experimental design in which the groups are cancer (HSC-3/sham) and drug treatment (propranolol, vehicle, GTD). Our sample size estimates are based on previous orofacial nociceptive behavior studies using the dolognawmeter assay[69; 96]; the endpoint is percent change in baseline gnaw-time. We hypothesized that drug treatment would reverse cancer-induced increase in gnaw-time by 70%. Effect size based on gnaw-time for the control group (vehicle/sham inoculation) and HSC-3 tumor-bearing mice was calculated and used in a power analysis to determine sample size needed to provide greater than 80% power to detect a change due to both cancer and drug treatment at $\alpha = .05$. Tumor volume outcome was not considered in sample size estimates for this study. Analysis of variance (ANOVA) was employed to evaluate the difference between groups regarding time and treatment. To adjust for multiple comparisons, the *post-hoc* Holm-Sidak test statistic was employed. Student's t test was employed to evaluate the difference between two groups. Pearson correlation coefficient was used to measure the linear relationship between two variables (i.e., gnaw-time and tumor area).

3.0 Results

3.1 Sympathetic post-ganglionic neurons innervate the oral cancer microenvironment

Perineural invasion correlates positively with a high degree of reported pain in patients with oral cancer[68]. Catecholamine precursor, tyrosine hydroxylase (TH) and sensory ion channel, transiet receptor potential vanilloid-1 (TRPV1), were used to identify putatively sympathetic and sensory neurons respectively innervating the tumor microenvironment in HNSCC patients, respectively. Anti-S100, a Schwann cell marker useful for evaluating nerve sheath, was used to identify peripheral nerve bundles in the tumor tissue. In serial sections, TH-immunoreactivity (IR) and TRPV1-IR fibers were found within S100-denoted nerve bundles suggesting a spatial relationship between these two fiber types within tumors (Figure 1A). Next, we quantified the percent of TH-IR and TRPV1-IR areas relative to total S100-IR nerve area in HNSCC tumor tissue across 13 patients. We found that TH-IR and TRPV1-IR nerve fibers comprise 4.34±1.4% and 18.03±4.0% of total S100-IR nerve area respectively (Figure 1B). We sought to define the potential role of sympathetic postganglionic neurons innervating the tongue in oral cancer pain. Using optical clearing and immunohistochemistry, we visualized TH-IR innervation in a naïve mouse tongue; while no vascular markers were used, TH-IR appears to be perivascular within the muscle and entering the mucosa (Figure 1C,D). Utilizing a xenograft mouse model of human tongue SCC in athymic nude mice, we identified TH-IR nerve bundles (Figure 1E) and perivascular TH-IR fibers (Figure 1F) innervating the tumor microenvironment. Similar to patient tissue data, we used serial coronal sections of mouse tongue tumor tissue to confirmed the spatial relationship between intratumoral putatively sympathetic and sensory nerve fibers (Suppl Figure 1). Furthermore, ten days following injection of retrograde tracer, DiI, into the C57Bl/6 mouse tongue, we found DiI-positive neurons in both the SCG, where cell bodies

give rise to the postganglionic sympathetic innervation of the head (Figure 1G), as well as the TG, where cell bodies give rise to sensory innervation of the head (Figure 2A). Previous reports have shown that TH is expressed in a subpopulation of sensory neurons in the adult mouse[14]. To address the possiblity that TH+ nerves innervating the mouse tongue tumor tissue are sensory in origin, we stained TG sections with retrograde labeling with anti-TH (9 sections/mouse, 3 male, 3 female mice). An average of 115.8.5±12.2 DiI+ neurons were counted per mouse and no significant overlap of TH-IR in DiI+ TGN innervating the tongue (0.73±0.4%) was detected (Figure 2A). Sympathetic neurons can regulate target organs by releasing NE, which activates adrenergic receptors[20]. In the muscle and skin, it has been shown that nociceptive activity can induce an increase in sympathetic discharge. However, the effect of sympathetic activity on nociceptive activity is debated[9; 31; 62]. To investigate this in the trigeminal system, we first sought to determine if TG express adrenergic receptors. Intact TG from both C57Bl/6 and athymic nude mice were probed for all α- and β- adrenergic subtypes using qPCR; genes for all receptor subtypes except *Adrb3* were expressed and there was no difference between the two genotypes (Table 1). Ganglia are comprised of multiple cell types, including satellite glia and immune cells both of which can express adrenergic genes[77; 81]. In order to assess tongue-innervating neuron-specific expression, ganglia from retrograde labeled mice (n=2 C57Bl/6 mice) were dissociated, and individual neurons were collected for single cell analysis based on fluorescence; cell size was not considered. RNA from 24 individual DiI-labeled neurons was subjected to qPCR analysis. All neurons tested contained detectable gene expression for at least 1 adrenergic receptor subtype (Figure 2B). α2-adrenergic subtypes were the most highly expressed (17/24 α-AR2a, 16/24 α-AR2b, 18/24 α-AR2c) followed by β-adrenergic subtypes (17/24 β-AR1, 10/24 β-AR2) (Figure 2C). The α1-adrenergic subtypes were expressed in the lowest percentage of neurons tested (5/24 α1-AR1a, 2/24 α1-AR1b, 1/24 α1-AR1d) (Figure 2C). Similar to whole ganglia PCR, β-AR3 was not expressed in any neuron tested. Next, we sought to determine if NE could evoke a functional response in neuronal activity in dissociated TGN that innervate the tongue. Microfluorimetry was used to quantify the evoked Ca^{2+} transient in response to 10μM NE application for 30s in dissociated TGN from 9 mice (5 C57Bl/6, 4 nude) with DiI retrograde labeling in the tongue (Figure 2D). We found that NE evoked a Ca^{2+} transient ≥20% of baseline intracellular Ca^{2+} concentration in 5.45% (3/55) DiI+ tongue TGN and 21.4% (28/131) non-tongue innervating neuron (DiI-negative) in the TG. The percent of responsive neurons per animal are depicted in Figure 2E.

3.2 β-AR2 is overexpressed in oral cancer cell lines

Previous studies have demonstrated that β-AR are more highly expressed in oral SCC compared to normal keratinocyte cells[76]. We used qPCR to determine the relative expression of β-AR 1, 2 and 3 in human oral cancer cell lines HSC-3 and SCC-4, benign human dysplastic oral keratinocyte cell line DOK, and immortalized human non-tumorigenic skin keratinocyte cell line HaCaT. Three separate passages of each cell line were tested, and the expression relative to β-actin was considered. *ADRB1* and *ADRB2* were highly expressed in oral cancer cell lines (HSC-3, SCC-4) and DOK compared to HaCaT (Figure 3A,B). *ADRB3* was not detected in any cell line tested. Two-way ANOVA found no significant interaction between relative gene expression and

cell line (F(3,16)=1.57, p=0.235). However, *ADRB2* expression was significantly higher than *ADRB1* expression in all cell lines (p<0.0001). We confirmed β-AR2 protein expression using immunohistochemistry in DOK, HSC-3, and SCC-4 cell lines. While protein expression was detected in all three cell lines, oral cancer cells appeared to have more expression in the plasma membrane than DOK (Figure 3C).

3.3 NE increases oral cancer cell proliferation and β-AR2 expression *in vitro*

Experimental analyses in animal models demonstrate that behavioral stress can accelerate growth in breast[84], pancreatic[39] and ovarian[86] cancer. To examine the effect of sympathetic neurotransmission on oral SCC cell proliferation and β-AR2 expression *in vitro*, HSC-3 and SCC-4 cells were treated with varying doses of NE and β-AR2 specific agonist, salbutamol; non-tumorigenic DOK cells served as a control. One-way ANOVA revealed that cell stimulation with 10μM NE for 24 hours resulted in a significant increase in HSC-3 (24.1±6.5%, p=0.002) and SCC-4 (32.2±8.6%, p=0.005) proliferation compared to cells stimulated with vehicle (0.05% HCl, 0.05% EtOH). Co-treatment with β-AR antagonist propranolol (10μM) blocked the NE-induced increase in cell proliferation; there was a significant decrease in proliferation in cells stimulated with NE+propranolol compared to cells stimulated with NE in both HSC-3 (−45.51±6.7%, p<0.0001) and SCC-4 (−48.18±5.8%, p=0.0003) (Figure 4A). Stimulation with 1μM salbutamol for 24 hours resulted in a significant increase only in SCC-4 (96.01±12.88%, p<0.0001) proliferation compared to cells stimulated with vehicle (0.1% H2O, 0.05% EtOH; One-way ANOVA). Co-treatment with propranolol (10μM) blocked the salbutamol-induced increase in cell proliferation; there was a significant difference in proliferation in cells stimulated with salbutamol+propranolol compared to cells stimulated with salbutamol in SCC-4 cell line (85.16±11.4%, p<0.0001) (Figure 4B) There was no significant effect on DOK proliferation after 24-hour treatment with 10μM NE (4.5±9.8%, p=0.658) or 1μM salbutamol (4.4±0.9%, p=0.830) (Figure 4B). We also measured β-AR2 protein expression in cell lines treated with vehicle, 1μM salbutamol and 10μM NE. One-way ANOVA revealed a significant increase in the number of cells with β-AR2 IR following 24-hour treatment with 10μM NE in HSC-3 (26.8±8.4%, p<0.0001) and SCC-4 (30.8±9.6%, p<0.0001) cell lines compared to vehicle (0.05% HCl, 0.1% H2O; Figure 4C,D). Stimulation with 1μM salbutamol for 24 hours resulted in a significant increase in the number of cells with β-AR2 IR in both HSC-3 (14.43±3.6%, p=0.039) and SCC-4 cell lines (29.54±9.2%, p=0.009) compared to vehicle (0.1% H2O; One-way ANOVA). Competitive β-AR2 agonist, ICI 118,551 (1μM) blocked the NE-induced increase in β-AR2 IR; there was a significant decrease in β-AR2 IR in cells stimulated with ICI 118,551+NE compared to cells stimulated with NE in both HSC-3 (−27.88±8.7%, p<0.0001) and SCC-4 (−41.77±13.1%, p<0.0001). There was no significant change in the number of β-AR2 immunoreactive cells following NE (1.71±0.5%, p=0.981) or salbutamol (0.28±0.1%, p=0.969) treatment in the DOK cell line compared to vehicle treatment (Figure 4C,D).

3.4 NE stimulation increases TNFα secretion from oral cancer cells *in vitro*

We previously demonstrated that TNFα secreted from cancer cells plays a role in oral SCC-induced nociceptive behavior[74]. Other investigators have demonstrated that NE-induced activation of cancer cells increases secretion of inflammatory cytokines and growth

factors[10; 91]. Consequently, we sought to determine if β-AR signaling altered TNFα protein secreted from oral cancer cells. We measured TNFα protein in SN from HSC-3, SCC-4 and DOK cells treated with vehicle (0.05% HCl, 0.05% EtOH, 0.1% H20), 10μM NE, or 10μM NE plus 10μM propranolol for 48 hours by ELISA. To investigate a specific role for β-AR2 specifically, we included β-AR2 specific agonist, salbutamol (1μM) as well as β-AR2 competitve antagonist, ICI 118, 551 (1μM). Receptor blocker was added 1 hour prior to agonists. There was significant interaction between treatment and cell lines tested (Two-way ANOVA $p<0.0001$, $F(10,36)=11.66$). TNFα protein concentration was significantly higher in HSC-3 and SCC-4 cells treated with 10μM NE ($p<0.0001$) and 1μM salbutamol ($p<0.0001$) compared to vehicle treatment (Figure 5A). There was also a significant difference in TNFα protein concentration between NE treatment and co-treated with 10μM NE + 10μM propranolol or 10μM NE + ICI 118,551 ($p<0.0001$) as well as a significant difference between 1μM salbutamol treatment compared to co-treatment with 1μM salbutamol + propranolol ($p<0.0001$) for both HSC-3 or SCC-4. Furthermore, there was no significant change in TNFα protein in SN from DOK cells after NE treatment compared to vehicle ($p=0.366$) (Figure 5A).

3.5 Tongue primary afferent neurons are activated by NE-stimulated oral cancer cell line SN

We previously demonstrated that mediators released from oral cancer cells directly activate dissociated TGN[74]; we hypothesize that this mechanism generates oral cancer-induced nociception. Furthermore, we found that primary afferent neurons innervating the tongue express two receptors for TNFα[74]. In this present study we sought to determine whether the NE-induced increase in TNFα secretion led to an increase in tongue (i.e., DiI+) TGN activation. We used microfluorimetry to quantify the evoked Ca^{2+} transients in retrograde labeled TGN from naïve C57Bl/6 mice in response to SN from oral cancer cell lines (HSC-3, SCC-4) or DOK. We used SN collected from cell culture following 48-hour incubation with vehicle (0.05% HCl, SN) or 10μM NE (SN+NE) (Figure 5B). We have previously demonstrated that TNF–TNFR signaling inhibitor C87, which directly binds to TNFα to block interaction with the receptor [50], was able to significantly reduce nociceptive behavior in two different oral cancer models[69; 74] and C87 reduced the HSC-3 secreted TNFα protein concentration as measured by ELISA[69]. To test the hypothesis that NE-evoked TNFα will modulate TGN activity, C87 was added to the SN at room temperature 15-20min prior to application. Application of SN+NE (4s) evoked a Ca^{2+} transient from significantly more TGN compared to SN from HSC-3 (33.81±10.4%, $p=0.008$) and SCC-4 (34.77±9.9%, $p=0.004$) (Figure 5C). Furthermore, SN+NE application evoked a Ca^{2+} transient with a significantly larger magnitude compared to SN from HSC-3 (145.71±20.6%, $p=0.035$) and SCC-4 (95.88±14.9%, $p=0.042$). There was no significant difference in the percent of responsive neurons or the evoked transient magnitude in response to DOK SN compared to DOK SN+NE (Figure 5C,D). Pre-treatment of C87 (1μM) in the bath solution for 1min followed by SN+NE+C87 application blocked the effects of NE-treated cell line SN on the evoked Ca^{2+} transient, as shown by the significant difference in the percent of responsive neurons (HSC-3:−121.11±23.5%, $p<0.0001$; SCC-4:−59.66±20.4%, $p=0.044$) and magnitude of the evoked Ca^{2+} transient

(HSC-3:−249.01±35.6, p=0.005; SCC-4:−130.22±39.65, p=0.020) for tongue TGN-treated with SN+NE+C87 compared to SN+NE for HSC-3 and SCC4 cell lines (Figure 5C, D).

3.6 Beta-blocker (propranolol) attenuated nociceptive behavior in a xenograft model of oral cancer

Antagonism of β-adrenergic signaling has been shown clinically to reduce the progression of several solid tumors[21], but its effect on oral cancer pain is unknown. HSC-3 orthotopic xenograft elicits orofacial nociceptive behavior in mice[71; 94]. We tested the hypothesis that β-AR antagonism would reduce oral cancer-induced nociceptive behavior by reducing TNFα secretion by the tumor. We chose to use the pan-antagonist, propranolol, given the data that β-AR2 specific agonist, salbutamol, was not as successful as NE at driving HSC-3 proliferation or TNFα secretion from HSC-3 cell line, suggesting a potential role for both β-ARs. Previous literature indicates that stress can modulate tumor growth and cancer pain in tumor-bearing animals, therefore, propranolol (0.25 g/L) was administered in the drinking water ad libitum, as previously reported[30; 79]. Baseline gnaw-times were quantified in parallel with dolognawmeters. Propranolol treatment, initiated at PID 3, had no significant effect on baseline gnaw-time in sham treated animals (Student's t test PID-8 vs PID 29, p=0.871). Two-way ANOVA treatment by time interaction ($p<0.0001$) revealed that propranolol exerted an analgesic effect during HSC-3 tumor progression. In tumor-bearing mice, propranolol treatment significantly reduced gnaw-time at PID 22 (p=0.0323), PID 26 (p=0.0015), and PID 29 ($p<0.0001$) compared to vehicle treatment (Figure 6A). Furthermore, while HSC-3 xenograft tumor resulted in a decrease in body weight over time (Two-way ANOVA interaction, p=0.0002), there was significantly less cancer-induced loss of body mass in propranolol-treated mice at PID 21 (p=0.043) and PID 28 (p=0.012) (Figure 6B). There was no significant effect of propranolol treatment on tumor size compared to vehicle treated mice (Student's t test, p=0.051, Figure 6C). Lastly, human TNFα concentration was quantified in homogenized tumor tissue from 10 tumor-bearing mice by ELISA and normalized to total protein isolated in the tongue sample. We found that tongue tumor tissue from propranolol-treated mice (50.1 ± 3.3 pg/ng, n=5) contained significantly less human TNFα compared to vehicle-treated mice (62.1 ± 1.72 pg/ng, n=5, Student's t test, p=0.006, Figure 6D).

3.7 Chemical sympathectomy attenuated nociceptive behavior and reduced tumor growth in a xenograft model of oral cancer

Next, we sought to target sympathetic neurotransmission directly by inhibiting NE release in the tumor microenvironment. We used GTD as a pharmacological agent to inhibit peripheral noradrenergic fibers by gradually depleting NE stores in nerve endings through competitive replacement in neurotransmitter vesicles[51]. GTD does not cross the blood-brain barrier[36] or accumulate in sensory nerves[34; 36]. Baseline gnaw-times were established in parallel in dolognawmeters; GTD (50mg/kg) was administered i.p. twice per week starting 1 week prior to inoculation; to limit stress, mice were injected directly prior to the dolognawmeter assay, a timepoint in which they are already being handled. GTD had no significant effect on gnaw-times in sham animals compared to vehicle (50ul saline) over time; these two groups were pooled. Similar to propranolol treatment, Two-way ANOVA treatment by time interaction ($p<0.0001$) revealed that GTD exerted an analgesic effect

during HSC-3 progression. In tumor-bearing mice, GTD treatment significantly reduced gnaw-time at PID 18 ($p=0.0005$) and PID 25 ($p=0.003$) compared to vehicle treated tumor-bearing mice (Figure 6E). While there was a decrease in body weight over time in tumor-bearing mice compared to sham (Two-way ANOVA interaction, $p<0.0001$), GTD treatment had no effect on cancer-induced loss of body mass in tumor-bearing mice at any time point (Figure 6F). We found that GTD treatment produced a significant reduction in tumor size (Student's t test, $p=0.0057$); GTD tumor-bearing mice had a significantly smaller tumor in the tongue compared to vehicle treated mice (Figure 6G). However, there was no correlation between tumor size and the percent change in gnaw-time at PID 28 in either the vehicle treatment group ($r=0.358$, $p=0.190$; Pearson Correlation; Suppl Figure 2) or GTD treatment group ($r=-0.137$, $p=0.625$; Pearson Correlation; Suppl Figure 2). Lastly, human TNFα concentration was quantified in homogenized tumor tissue from 10 tumor-bearing mice by ELISA and normalized to total protein isolated in the tongue sample. We found no significant difference in human TNFα in tongue tumor tissue from GTD-treated mice (54.2 ± 2.5 pg/ng, n=5) and vehicle-treated mice (61.7 ± 3.71 pg/ng, n=5, Student's t test, $p=0.072$, Figure 6H).

4.0 Discussion:

Oral cancer patients can have extreme psychological distress [17] and pain[22; 40] at diagnosis and beyond treatment[4; 47]. Circulating NE levels were higher in HNSCC patients versus patients with benign oral lesions, and intratumor NE levels correlate positively with psychosocial risk factors[49]. Preclinical models have shown that chronic stress can increase sympathetic nerve fiber growth and branching into the periphery while upregulating adrenergic basal activity in target tissue[83]. Here, we hypothesize sympathetic modulation of oral cancer pain via direct NE activation of oral cancer cells results in TNFα secretion and consequential primary afferent sensitization (Figure 7). We found TH-IR sympathetic and TRPV1-IR sensory nerves innervating tumors from 9 of 13 patients with tongue SCC. TRPV1 was used to identify sensory nerves as it is expressed in greater than 90% of human sensory neurons[57]. While we and others have previously demonstrated a sex difference in HNSCC pain reports[66; 72], we found no sex difference in tumor nerve presence, although the sample size was small. Three of the four patients lacking TH-IR had HPV-positive tumors, which show biological differences (i.e., anatomical involvement[37], extracellular vesicle release[27]) associated with less innervation and reduced symptom burden. Additionally, these HPV-positive tumors reside in the oropharynx region; the anatomic subsite and demographics vary between oropharyngeal and oral cavity SCC with the former having a lower density of nerve fibers[58].

Previous assessment of mRNA in the dorsal root ganglion (DRG) indicates that primary afferent neurons possess several types of α-adrenoceptors[53; 78; 90]. While intact nociceptive primary afferent neurons show insignificant response to sympathetic activiy in muscle and skin[32], *in vitro* evidence suggests α1-AR activation can increase sensory neuron excitability[9; 18]. This study, along with recent findings wherein trigeminal afferent fibers showed decreased threshold in response to α1-AR agonist phenylephrine[8], suggest direct adrenergic influence on nociceptive signaling. Our data found that tongue-innervating TGN express mainly α2-ARs, and NE did not evoke a Ca^{2+} transient in the majority of

dissociated tongue-innervating TGN from naïve mice. However, it is possible that following inflammation or injury, NE and sympathetic stimulation could result in increased excitability in nociceptive afferents[2; 13; 70]. The single-cell PCR results support co-expression of multiple subtypes of both α- and β-ARs within the same neuron[24], likely contributing to variability with injury over time[12; 54]. While α-AR are the most studied in peripheral sensory neurons, β-AR antagonism (i.e., beta-blockers) is associated with lower prevalence of joint pain and lower opioid requirement in patients with osteoarthritis[88]. Debate persists regarding which adrenergic subtype(s) most greatly influence pain, and additional studies must investigate TGN plasticity in adrenergic subtypes.

Previous studies have shown that catecholamines broadly enhance cancer cell expression of proteins and enzymes known to influence tumor progression[7; 28; 91], although pain was not assessed. Sympathetic postganglionic neurons have been implicated in pain via α2-AR mediated release of prostaglandin E2 (PGE2)[25]. While PGE2–mediated inflammation is possibly linked to oral cancer development and progression [59], it has not yet been implicated in oral cancer pain. Alternatively, TNFα is an important regulator of oral cancer pain[69; 74], and its receptors, TNFRI and TNFRII, are expressed by the majority of tongue-innervating sensory neurons[74]. We have previously shown that the TNF-TNFR blocker C87 reduced nociceptive behavior in a carcinogen-induced oral cancer mouse model[69]. Here, we demonstrate that NE or salbutamol treatment in oral cancer cell lines evoked a significant increase in TNFα release. Baik et al. found elevated TNF-IR in nerves from rats with mechanical hyperalgesia in response to intradermal NE, suggesting that adrenergic activity is related to TNF signaling in the nerve[5]. While the increased magnitude of the response of tongue-innervating TGN to SN+NE treatment aligns with other data, the increase in percent responsive neurons was surprising, given that 30sec application was unlikely to have altered TNFR expression or threshold. However, since the transient response is not large, the treatment might have increased a previously undetectably small response above the threshold of detection. We therefore infer that NE-evoked TNFα release can activate nociceptive neurons and subsequently sensitize neurons within the tumor.

Chronic stress promotes oral cancer growth and angiogenesis in mouse and rat models of oral cancer. Here, we found that propranolol ingestion significantly reduced orofacial nociceptive behavior and TNFα protein in mouse tongue tumors. We chose to use a non-selective β-AR antagonist given the *in vitro* data that specific β-AR2 activation using salbutamol was unable to recapitulate the NE-induced proliferation in HSC-3 cells, suggesting that both β1 and β2 receptors may contribute to the NE-mediated effects on cancer proliferation. Since propranolol has a half life from 3 to 6 hours and a large volume of distribution (4 L/kg), multiple doses are required to achieve therapeutic effect[1]. Given evidence that stress impacts tumor growth[39; 44], we chose to avoid a daily multi-dose injection regimen and administered propranolol in the drinking water *ad libitum,* as has been done previously[30; 79]. We recognize that this route of administration presents several limitations, most notably the potential variability in bioavailability among mice and over time.

Cecilio and colleagues recently demonstrated that subcutaneous delivery of propranolol (3mg/day) inhibited oral carcinogenesis and reduced tumor invasion in a rat carcinogen

model of oral cancer[15]. We did not detect a significant difference in tumor size between tumor-bearing mice that received vehicle or propranolol; the lack of tumor reduction may be due to administration route. However, the reduction in human TNFα in the tongue suggests peripheral action of propranolol locally in the tumor. The anti-nociceptive effects observed in propranolol-treated tumor-bearing mice are hypothesized to be due to a reduction in tumor cell TNFα secretion. These data are supported by *in vitro* findings that propranolol inhibited NE-induced secretion of TNFα in oral cancer cell lines and TNF-TNFR inhibition blocked the increase in sensory neuron response to NE-treated cancer cell line supernatant. We also found a reduction in cancer-induced weight loss in tumor-bearing mice treated with propranolol compared to vehicle treatment. While propranolol actions appear to be peripheral, it is possible that centrally mediated anxiolytic effects contributed to the gnawing behavior and weight gain. However, previous reports indicate no difference in anxiety-like behaviors in oral cancer-bearing mice compared to sham[93]. Feeding behavior and body weight have been previously used as an index for nociception; analgesics in tumor-bearing mice reduced oral cancer-mediated weight loss[19]. While we did not directly measure feeding behavior, the increased body weight in propranolol-treated tumor-bearing mice suggests a reduction in orofacial nociception.

Sympathetic denervation has been shown to decrease tumor size in a rat tongue cancer model[64]. We found that chemical sympathecotomy via GTD treatment significantly reduced orofacial nociceptive behavior and tumor size compared to vehicle treatment in tumor-bearing mice. One week prior to inoculation, this agent was administered i.p. twice a week, given the half-life (~1.5 days), lack of stability in water, and previous reports[80]. Tumor-bearing mice treated with GTD also had significantly smaller tumors but no change in tumor TNFα concentration. Loss of NE-induced tumor cell proliferation could explain the tumor size reduction in GTD-treated mice. It is also possible that GTD-induced NE depletion also reduced tumor angiogenesis, leading to necrosis from intratumor hypoxia[87] and subsequent tumor reduction as well as release of intracellular protein (i.e. TNFα) [56]. Though nociceptive behavior was significantly reduced in GTD mice compared to vehicle treatment, the lack of improvement in weight loss suggests that some cancer pain persisted. Previous reports in bone cancer pain have demonstrated that tumor burden within the bone causes breakthrough pain with properties of ongoing pain[46]. We found no correlation between tumor size and the percent change in gnaw-time at PID 29, thus we are unable to associate the reduction in cancer-induced nociceptive behavior with tumor size. Previously published clinical [22] and preclinical [94] data indicated that oral cancer pain is exacerbated by function and is not correlated with tumor size; even the smallest oral cancers can produce severe pain. However, it is possible that loss of NE-induced tumor cell proliferation delayed the onset of orofacial nociception in GTD-treated tumor-bearing mice. Thus, these data suggest that chemical sympathectomy modulated oral cancer progression and pain, independent of TNFα.

Currently, prospective clinical trials are investigating the therapeutic value of beta blockers in prostate (NCT02944201), gastrointestinal (NCT03245554), and breast (NCT01847001) cancers along with melanoma (NCT02962947). However, patient-reported pain is not assessed in these trials. Despite well documented pain and stress in HNSCC patients, the impact of adrenergic signaling on SCC pain and progression is unknown. The data here

suggest that sympathetic input may impact oral cancer pain development via TNFα as well as tumor progression. However, further studies are needed to determine the therapeutic use of β-adrenergic antagonism in the treatment of established oral cancer pain. Given that β-adrenergic signaling can functionally suppress T cells and natural killer cells[84], β-adrenergic blockage could exert a dual effect to reduce both the SNS-related maintenance of cancer pain and the suppression of immune response to tumor progression. Further investigations into β-adrenergic antagonism using immunocompetant mice could elucidate such a synergistic approach, potentially improving both quality of life and symptom management for HNSCC patients.

Supplementary Material

Refer to Web version on PubMed Central for supplementary material.

Acknowledgements:

We thank the Hillman Cancer Center Head and Neck Tissue Bank for suppling clinical specimens as well as Dr. Elizabeth Bilodeau DMD, MD, MSEd for her expertise in pathological assessment of the HNSCC tumor tissue. We thank the University of Pittsburgh Center for Biologic Imaging for their technical support in imaging the mouse tongue tissue.

Funding:

This work was supported by the National Institute of Dental and Craniofacial Research through individual investigator grants R00DE028019 and R01DE030892 (NNS, senior author) as well as R01DE026806 and R01DE029951 (BLS). We acknowledge the UPMC Hillman Cancer Center and Tissue and Research Pathology/Pitt Biospecimen Core shared resource which is supported in part by award P30CA047904.

Bibliography

[1]. Al Shaker HA, Qinna NA, Badr M, Al Omari MMH, Idkaidek N, Matalka KZ, Badwan AA. Glucosamine modulates propranolol pharmacokinetics via intestinal permeability in rats. Eur J Pharm Sci 2017;105:137–143. [PubMed: 28502673]

[2]. Ali Z, Ringkamp M, Hartke TV, Chien HF, Flavahan NA, Campbell JN, Meyer RA. Uninjured C-fiber nociceptors develop spontaneous activity and alpha-adrenergic sensitivity following L6 spinal nerve ligation in monkey. J Neurophysiol 1999;81(2):455–466. [PubMed: 10036297]

[3]. Amit M, Takahashi H, Dragomir MP, Lindemann A, Gleber-Netto FO, Pickering CR, Anfossi S, Osman AA, Cai Y, Wang R, Knutsen E, Shimizu M, Ivan C, Rao X, Wang J, Silverman DA, Tam S, Zhao M, Caulin C, Zinger A, Tasciotti E, Dougherty PM, El-Naggar A, Calin GA, Myers JN. Loss of p53 drives neuron reprogramming in head and neck cancer. Nature 2020;578(7795):449–454. [PubMed: 32051587]

[4]. Ates O, Soylu C, Babacan T, Sarici F, Kertmen N, Allen D, Sever AR, Altundag K. Assessment of psychosocial factors and distress in women having adjuvant endocrine therapy for breast cancer: the relationship among emotional distress and patient and treatment-related factors. Springerplus 2016;5:486. [PubMed: 27218001]

[5]. Baik E, Chung JM, Chung K. Peripheral norepinephrine exacerbates neuritis-induced hyperalgesia. J Pain 2003;4(4):212–221. [PubMed: 14622706]

[6]. Banik RK, Sato J, Giron R, Yajima H, Mizumura K. Interactions of bradykinin and norepinephrine on rat cutaneous nociceptors in both normal and inflamed conditions in vitro. Neurosci Res 2004;49(4):421–425. [PubMed: 15236868]

[7]. Barbieri A, Bimonte S, Palma G, Luciano A, Rea D, Giudice A, Scognamiglio G, La Mantia E, Franco R, Perdona S, De Cobelli O, Ferro M, Zappavigna S, Stiuso P, Caraglia M, Arra C. The stress hormone norepinephrine increases migration of prostate cancer cells in vitro and in vivo. Int J Oncol 2015;47(2):527–534. [PubMed: 26058426]

[8]. Bastos DB, Sarafim-Silva BAM, Sundefeld M, Ribeiro AA, Brandao JDP, Biasoli ER, Miyahara GI, Casarini DE, Bernabe DG. Circulating catecholamines are associated with biobehavioral factors and anxiety symptoms in head and neck cancer patients. PLoS One 2018;13(8):e0202515. [PubMed: 30125310]

[9]. Benbow T, Ranjbar Ekbatan M, Cairns BE. alpha1 adrenergic receptor activation has a dynamic effect on masticatory muscle afferent fibers. Neuropharmacology 2020;175:108197. [PubMed: 32544482]

[10]. Bernabe DG, Tamae AC, Biasoli ER, Oliveira SH. Stress hormones increase cell proliferation and regulates interleukin-6 secretion in human oral squamous cell carcinoma cells. Brain Behav Immun 2011;25(3):574–583. [PubMed: 21187140]

[11]. Bicanic I, Hladnik A, Dzaja D, Petanjek Z. The Anatomy of Orofacial Innervation. Acta Clin Croat 2019;58(Suppl 1):35–42. [PubMed: 31741557]

[12]. Birder LA, Perl ER. Expression of alpha2-adrenergic receptors in rat primary afferent neurones after peripheral nerve injury or inflammation. J Physiol 1999;515 (Pt 2):533–542. [PubMed: 10050019]

[13]. Bossut DF, Perl ER. Effects of nerve injury on sympathetic excitation of A delta mechanical nociceptors. J Neurophysiol 1995;73(4):1721–1723. [PubMed: 7643179]

[14]. Brumovsky P, Villar MJ, Hokfelt T. Tyrosine hydroxylase is expressed in a subpopulation of small dorsal root ganglion neurons in the adult mouse. Exp Neurol 2006;200(1):153–165. [PubMed: 16516890]

[15]. Cecilio HP, Valente VB, Pereira KM, Kayahara GM, Furuse C, Biasoli ER, Miyahara GI, Oliveira SHP, Bernabe DG. Beta-adrenergic blocker inhibits oral carcinogenesis and reduces tumor invasion. Cancer Chemother Pharmacol 2020;86(5):681–686. [PubMed: 32980903]

[16]. Chen AM, Jennelle RL, Grady V, Tovar A, Bowen K, Simonin P, Tracy J, McCrudden D, Stella JR, Vijayakumar S. Prospective study of psychosocial distress among patients undergoing radiotherapy for head and neck cancer. Int J Radiat Oncol Biol Phys 2009;73(1):187–193. [PubMed: 18513884]

[17]. Chen SC, Liao CT, Lin CC, Chang JT, Lai YH. Distress and care needs in newly diagnosed oral cavity cancer patients receiving surgery. Oral Oncol 2009;45(9):815–820. [PubMed: 19250858]

[18]. Chen X, Levine JD. Epinephrine-induced excitation and sensitization of rat C-fiber nociceptors. J Pain 2005;6(7):439–446. [PubMed: 15993822]

[19]. Chodroff L, Bendele M, Valenzuela V, Henry M, Ruparel S. EXPRESS: BDNF Signaling Contributes to Oral Cancer Pain in a Preclinical Orthotopic Rodent Model. Mol Pain 2016;12.

[20]. Cole SW, Nagaraja AS, Lutgendorf SK, Green PA, Sood AK. Sympathetic nervous system regulation of the tumour microenvironment. Nat Rev Cancer 2015;15(9):563–572. [PubMed: 26299593]

[21]. Cole SW, Sood AK. Molecular pathways: beta-adrenergic signaling in cancer. Clin Cancer Res 2012;18(5):1201–1206. [PubMed: 22186256]

[22]. Connelly ST, Schmidt BL. Evaluation of pain in patients with oral squamous cell carcinoma. J Pain 2004;5(9):505–510. [PubMed: 15556829]

[23]. Dolan JC, Lam DK, Achdjian SH, Schmidt BL. The dolognawmeter: a novel instrument and assay to quantify nociception in rodent models of orofacial pain. J Neurosci Methods 2010;187(2):207–215. [PubMed: 20096303]

[24]. Gold MS, Dastmalchi S, Levine JD. Alpha 2-adrenergic receptor subtypes in rat dorsal root and superior cervical ganglion neurons. Pain 1997;69(1-2):179–190. [PubMed: 9060029]

[25]. Gonzales R, Sherbourne CD, Goldyne ME, Levine JD. Noradrenaline-induced prostaglandin production by sympathetic postganglionic neurons is mediated by alpha 2-adrenergic receptors. J Neurochem 1991;57(4):1145–1150. [PubMed: 1654387]

[26]. Grynkiewicz G, Poenie M, Tsien RY. A new generation of Ca2+ indicators with greatly improved fluorescence properties. J Biol Chem 1985;260(6):3440–3450. [PubMed: 3838314]

[27]. Guenat D, Hermetet F, Pretet JL, Mougin C. Exosomes and Other Extracellular Vesicles in HPV Transmission and Carcinogenesis. Viruses 2017;9(8).

[28]. Guo K, Ma Q, Wang L, Hu H, Li J, Zhang D, Zhang M. Norepinephrine-induced invasion by pancreatic cancer cells is inhibited by propranolol. Oncol Rep 2009;22(4):825–830. [PubMed: 19724861]

[29]. Haggard P, de Boer L. Oral somatosensory awareness. Neurosci Biobehav Rev 2014;47:469–484. [PubMed: 25284337]

[30]. Hasegawa H, Saiki I. Psychosocial stress augments tumor development through beta-adrenergic activation in mice. Jpn J Cancer Res 2002;93(7):729–735. [PubMed: 12149137]

[31]. Horeyseck G, Janig W. Reflexes in postganglionic fibres within skin and muscle nerves after noxious stimulation of skin. Exp Brain Res 1974;20(2):125–134. [PubMed: 4837736]

[32]. Horeyseck G, Thamer V. [Methylprednisolone-induced inhibition of the sympathetic vasomotor tonus in hemorrhagic shock]. Chir Forum Exp Klin Forsch 1978(1978):65–68. [PubMed: 222554]

[33]. Ito J, Oyagi S. Determination of the origin of autonomic nerves of the tongue using horseradish peroxidase as tracer. Eur Arch Otorhinolaryngol 1994;251(2):117–118. [PubMed: 8024759]

[34]. Jensen-Holm J, Juul P. Ultrastructural changes in the rat superior cervical ganglion following prolonged guanethidine administration. Acta Pharmacol Toxicol (Copenh) 1971;30(3):308–320. [PubMed: 5171947]

[35]. Jing D, Zhang S, Luo W, Gao X, Men Y, Ma C, Liu X, Yi Y, Bugde A, Zhou BO, Zhao Z, Yuan Q, Feng JQ, Gao L, Ge WP, Zhao H. Tissue clearing of both hard and soft tissue organs with the PEGASOS method. Cell Res 2018;28(8):803–818. [PubMed: 29844583]

[36]. Johnson EM Jr., Manning PT. Guanethidine-induced destruction of sympathetic neurons. Int Rev Neurobiol 1984;25:1–37. [PubMed: 6206012]

[37]. Kato MG, Baek CH, Chaturvedi P, Gallagher R, Kowalski LP, Leemans CR, Warnakulasuriya S, Nguyen SA, Day TA. Update on oral and oropharyngeal cancer staging - International perspectives. World J Otorhinolaryngol Head Neck Surg 2020;6(1):66–75. [PubMed: 32426706]

[38]. Katz MR, Kopek N, Waldron J, Devins GM, Tomlinson G. Screening for depression in head and neck cancer. Psychooncology 2004;13(4):269–280. [PubMed: 15054731]

[39]. Kim-Fuchs C, Le CP, Pimentel MA, Shackleford D, Ferrari D, Angst E, Hollande F, Sloan EK. Chronic stress accelerates pancreatic cancer growth and invasion: a critical role for beta-adrenergic signaling in the pancreatic microenvironment. Brain Behav Immun 2014;40:40–47. [PubMed: 24650449]

[40]. Kolokythas A, Connelly ST, Schmidt BL. Validation of the University of California San Francisco Oral Cancer Pain Questionnaire. J Pain 2007;8(12):950–953. [PubMed: 17686656]

[41]. Kugaya A, Akechi T, Okuyama T, Nakano T, Mikami I, Okamura H, Uchitomi Y. Prevalence, predictive factors, and screening for psychologic distress in patients with newly diagnosed head and neck cancer. Cancer 2000;88(12):2817–2823. [PubMed: 10870066]

[42]. Kulik G ADRB2-Targeting Therapies for Prostate Cancer. Cancers (Basel) 2019;11(3).

[43]. Kurita GP, Sjogren P, Klepstad P, Mercadante S. Interventional Techniques to Management of Cancer-Related Pain: Clinical and Critical Aspects. Cancers (Basel) 2019;11(4).

[44]. Lamkin DM, Sloan EK, Patel AJ, Chiang BS, Pimentel MA, Ma JC, Arevalo JM, Morizono K, Cole SW. Chronic stress enhances progression of acute lymphoblastic leukemia via beta-adrenergic signaling. Brain Behav Immun 2012;26(4):635–641. [PubMed: 22306453]

[45]. Lindsay TH, Jonas BM, Sevcik MA, Kubota K, Halvorson KG, Ghilardi JR, Kuskowski MA, Stelow EB, Mukherjee P, Gendler SJ, Wong GY, Mantyh PW. Pancreatic cancer pain and its correlation with changes in tumor vasculature, macrophage infiltration, neuronal innervation, body weight and disease progression. Pain 2005;119(1-3):233–246. [PubMed: 16298491]

[46]. Lozano-Ondoua AN, Symons-Liguori AM, Vanderah TW. Cancer-induced bone pain: Mechanisms and models. Neurosci Lett 2013;557 Pt A:52–59. [PubMed: 24076008]

[47]. Lutgendorf SK, Andersen BL. Biobehavioral approaches to cancer progression and survival: Mechanisms and interventions. Am Psychol 2015;70(2):186–197. [PubMed: 25730724]

[48]. Lutgendorf SK, Cole S, Costanzo E, Bradley S, Coffin J, Jabbari S, Rainwater K, Ritchie JM, Yang M, Sood AK. Stress-related mediators stimulate vascular endothelial growth factor secretion by two ovarian cancer cell lines. Clin Cancer Res 2003;9(12):4514–4521. [PubMed: 14555525]

[49]. Lutgendorf SK, DeGeest K, Sung CY, Arevalo JM, Penedo F, Lucci J, 3rd, Goodheart M, Lubaroff D, Farley DM, Sood AK, Cole SW. Depression, social support, and beta-adrenergic transcription control in human ovarian cancer. Brain Behav Immun 2009;23(2):176–183. [PubMed: 18550328]

[50]. Ma L, Gong H, Zhu H, Ji Q, Su P, Liu P, Cao S, Yao J, Jiang L, Han M, Ma X, Xiong D, Luo HR, Wang F, Zhou J, Xu Y. A novel small-molecule tumor necrosis factor alpha inhibitor attenuates inflammation in a hepatitis mouse model. J Biol Chem 2014;289(18):12457–12466. [PubMed: 24634219]

[51]. Manning PT, Powers CW, Schmidt RE, Johnson EM, Jr. Guanethidine-induced destruction of peripheral sympathetic neurons occurs by an immune-mediated mechanism. J Neurosci 1983;3(4):714–724. [PubMed: 6131947]

[52]. Mantyh WG, Jimenez-Andrade JM, Stake JI, Bloom AP, Kaczmarska MJ, Taylor RN, Freeman KT, Ghilardi JR, Kuskowski MA, Mantyh PW. Blockade of nerve sprouting and neuroma formation markedly attenuates the development of late stage cancer pain. Neuroscience 2010;171(2):588–598. [PubMed: 20851743]

[53]. Maruo K, Yamamoto H, Yamamoto S, Nagata T, Fujikawa H, Kanno T, Yaguchi T, Maruo S, Yoshiya S, Nishizaki T. Modulation of P2X receptors via adrenergic pathways in rat dorsal root ganglion neurons after sciatic nerve injury. Pain 2006;120(1-2):106–112. [PubMed: 16360272]

[54]. Michaelis M, Devor M, Janig W. Sympathetic modulation of activity in rat dorsal root ganglion neurons changes over time following peripheral nerve injury. J Neurophysiol 1996;76(2):753–763. [PubMed: 8871196]

[55]. Moayedi Y, Duenas-Bianchi LF, Lumpkin EA. Somatosensory innervation of the oral mucosa of adult and aging mice. Sci Rep 2018;8(1):9975. [PubMed: 29967482]

[56]. Montfort A, Colacios C, Levade T, Andrieu-Abadie N, Meyer N, Segui B. The TNF Paradox in Cancer Progression and Immunotherapy. Front Immunol 2019;10:1818. [PubMed: 31417576]

[57]. Moy JK, Hartung JE, Duque MG, Friedman R, Nagarajan V, Loeza-Alcocer E, Koerber HR, Christoph T, Schroder W, Gold MS. Distribution of functional opioid receptors in human dorsal root ganglion neurons. Pain 2020;161(7):1636–1649. [PubMed: 32102022]

[58]. Mu L, Sanders I. Sensory nerve supply of the human oro- and laryngopharynx: a preliminary study. Anat Rec 2000;258(4):406–420. [PubMed: 10737859]

[59]. Nasry WHS, Rodriguez-Lecompte JC, Martin CK. Role of COX-2/PGE2 Mediated Inflammation in Oral Squamous Cell Carcinoma. Cancers (Basel) 2018;10(10).

[60]. Pasquier E, Ciccolini J, Carre M, Giacometti S, Fanciullino R, Pouchy C, Montero MP, Serdjebi C, Kavallaris M, Andre N. Propranolol potentiates the anti-angiogenic effects and anti-tumor efficacy of chemotherapy agents: implication in breast cancer treatment. Oncotarget 2011;2(10):797–809. [PubMed: 22006582]

[61]. Pertovaara A The noradrenergic pain regulation system: a potential target for pain therapy. Eur J Pharmacol 2013;716(1-3):2–7. [PubMed: 23500194]

[62]. Pluteanu F, Ristoiu V, Flonta ML, Reid G. Alpha(1)-adrenoceptor-mediated depolarization and beta-mediated hyperpolarization in cultured rat dorsal root ganglion neurones. Neurosci Lett 2002;329(3):277–280. [PubMed: 12183030]

[63]. Pohto P Sympathetic adrenergic innervation of permanent teeth in the monkey (Macaca irus). Acta Odontol Scand 1972;30(1):117–126. [PubMed: 4624791]

[64]. Raju B, Hultstrom M, Haug SR, Ibrahim SO, Heyeraas KJ. Sympathectomy suppresses tumor growth and alters gene-expression profiles in rat tongue cancer. Eur J Oral Sci 2009;117(4):351–361. [PubMed: 19627344]

[65]. Raju B, Ibrahim SO. Pathophysiology of oral cancer in experimental animal models: a review with focus on the role of sympathetic nerves. J Oral Pathol Med 2011;40(1):1–9. [PubMed: 20819130]

[66]. Reyes-Gibby CC, Anderson KO, Merriman KW, Todd KH, Shete SS, Hanna EY. Survival patterns in squamous cell carcinoma of the head and neck: pain as an independent prognostic factor for survival. J Pain 2014;15(10):1015–1022. [PubMed: 25043982]

[67]. Ricon I, Hanalis-Miller T, Haldar R, Jacoby R, Ben-Eliyahu S. Perioperative biobehavioral interventions to prevent cancer recurrence through combined inhibition of beta-adrenergic and cyclooxygenase 2 signaling. Cancer 2019;125(1):45–56. [PubMed: 30291805]

[68]. Salvo E, Campana WM, Scheff NN, Nguyen TH, Jeong SH, Wall I, Wu AK, Zhang S, Kim H, Bhattacharya A, Janal MN, Liu C, Albertson DG, Schmidt BL, Dolan JC, Schmidt RE, Boada MD, Ye Y. Peripheral nerve injury and sensitization underlie pain associated with oral cancer perineural invasion. Pain 2020;161(11):2592–2602. [PubMed: 32658150]

[69]. Salvo E, Tu NH, Scheff NN, Dubeykovskaya ZA, Chavan SA, Aouizerat BE, Ye Y. TNFalpha promotes oral cancer growth, pain, and Schwann cell activation. Sci Rep 2021;11(1):1840. [PubMed: 33469141]

[70]. Sato J, Perl ER. Adrenergic excitation of cutaneous pain receptors induced by peripheral nerve injury. Science 1991;251(5001):1608–1610. [PubMed: 2011742]

[71]. Scheff NN, Alemu RG, Klares R 3rd, Wall IM, Yang SC, Dolan JC, Schmidt BL. Granulocyte-Colony Stimulating Factor-Induced Neutrophil Recruitment Provides Opioid-Mediated Endogenous Anti-nociception in Female Mice With Oral Squamous Cell Carcinoma. Front Mol Neurosci 2019;12:217. [PubMed: 31607857]

[72]. Scheff NN, Bhattacharya A, Dowse E, Dang RX, Dolan JC, Wang S, Kim H, Albertson DG, Schmidt BL. Neutrophil-Mediated Endogenous Analgesia Contributes to Sex Differences in Oral Cancer Pain. Front Integr Neurosci 2018;12:52. [PubMed: 30405367]

[73]. Scheff NN, Lu SG, Gold MS. Contribution of endoplasmic reticulum Ca2+ regulatory mechanisms to the inflammation-induced increase in the evoked Ca2+ transient in rat cutaneous dorsal root ganglion neurons. Cell Calcium 2013;54(1):46–56. [PubMed: 23642703]

[74]. Scheff NN, Ye Y, Bhattacharya A, MacRae J, Hickman DN, Sharma AK, Dolan JC, Schmidt BL. Tumor necrosis factor alpha secreted from oral squamous cell carcinoma contributes to cancer pain and associated inflammation. Pain 2017;158(12):2396–2409. [PubMed: 28885456]

[75]. Schuller C, Kanel N, Muller O, Kind AB, Tinner EM, Hosli I, Zimmermann R, Surbek D. Stress and pain response of neonates after spontaneous birth and vacuum-assisted and cesarean delivery. Am J Obstet Gynecol 2012;207(5):416 e411–416.

[76]. Shang ZJ, Liu K, Liang DF. Expression of beta2-adrenergic receptor in oral squamous cell carcinoma. J Oral Pathol Med 2009;38(4):371–376. [PubMed: 19141064]

[77]. Shen S, Tiwari N, Madar J, Mehta P, Qiao LY. beta2 adrenergic receptor mediates noradrenergic action to induce CREB phosphorylation in satellite glial cells of dorsal root ganglia to regulate visceral hypersensitivity. Pain 2021.

[78]. Shi TS, Winzer-Serhan U, Leslie F, Hokfelt T. Distribution and regulation of alpha(2)-adrenoceptors in rat dorsal root ganglia. Pain 2000;84(2-3):319–330. [PubMed: 10666537]

[79]. Shimizu Y, Hosomichi J, Kaneko S, Shibutani N, Ono T. Effect of sympathetic nervous activity on alveolar bone loss induced by occlusal hypofunction in rats. Arch Oral Biol 2011;56(11):1404–1411. [PubMed: 21658677]

[80]. Shir Y, Seltzer Z. Effects of sympathectomy in a model of causalgiform pain produced by partial sciatic nerve injury in rats. Pain 1991;45(3):309–320. [PubMed: 1876441]

[81]. Simpson RJ, Bosslau TK, Weyh C, Niemiro GM, Batatinha H, Smith KA, Kruger K. Exercise and adrenergic regulation of immunity. Brain Behav Immun 2021.

[82]. Singer S, Krauss O, Keszte J, Siegl G, Papsdorf K, Severi E, Hauss J, Briest S, Dietz A, Brahler E, Kortmann RD. Predictors of emotional distress in patients with head and neck cancer. Head Neck 2012;34(2):180–187. [PubMed: 21400629]

[83]. Sloan EK, Capitanio JP, Tarara RP, Mendoza SP, Mason WA, Cole SW. Social stress enhances sympathetic innervation of primate lymph nodes: mechanisms and implications for viral pathogenesis. J Neurosci 2007;27(33):8857–8865. [PubMed: 17699667]

[84]. Sloan EK, Priceman SJ, Cox BF, Yu S, Pimentel MA, Tangkanangnukul V, Arevalo JM, Morizono K, Karanikolas BD, Wu L, Sood AK, Cole SW. The sympathetic nervous system induces a metastatic switch in primary breast cancer. Cancer Res 2010;70(18):7042–7052. [PubMed: 20823155]

[85]. Sood AK, Bhatty R, Kamat AA, Landen CN, Han L, Thaker PH, Li Y, Gershenson DM, Lutgendorf S, Cole SW. Stress hormone-mediated invasion of ovarian cancer cells. Clin Cancer Res 2006;12(2):369–375. [PubMed: 16428474]

[86]. Thaker PH, Han LY, Kamat AA, Arevalo JM, Takahashi R, Lu C, Jennings NB, Armaiz-Pena G, Bankson JA, Ravoori M, Merritt WM, Lin YG, Mangala LS, Kim TJ, Coleman RL, Landen CN, Li Y, Felix E, Sanguino AM, Newman RA, Lloyd M, Gershenson DM, Kundra V, Lopez-Berestein G, Lutgendorf SK, Cole SW, Sood AK. Chronic stress promotes tumor growth and angiogenesis in a mouse model of ovarian carcinoma. Nat Med 2006;12(8):939–944. [PubMed: 16862152]

[87]. Tilan J, Kitlinska J. Sympathetic Neurotransmitters and Tumor Angiogenesis-Link between Stress and Cancer Progression. J Oncol 2010;2010:539706. [PubMed: 20508839]

[88]. Valdes AM, Abhishek A, Muir K, Zhang W, Maciewicz RA, Doherty M. Association of Beta-Blocker Use With Less Prevalent Joint Pain and Lower Opioid Requirement in People With Osteoarthritis. Arthritis Care Res (Hoboken) 2017;69(7):1076–1081. [PubMed: 27696728]

[89]. Vickers ER, Cousins MJ. Neuropathic orofacial pain. Part 2-Diagnostic procedures, treatment guidelines and case reports. Aust Endod J 2000;26(2):53–63. [PubMed: 11359283]

[90]. Xie J, Ho Lee Y, Wang C, Mo Chung J, Chung K. Differential expression of alpha1-adrenoceptor subtype mRNAs in the dorsal root ganglion after spinal nerve ligation. Brain Res Mol Brain Res 2001;93(2):164–172. [PubMed: 11589993]

[91]. Yang EV, Kim SJ, Donovan EL, Chen M, Gross AC, Webster Marketon JI, Barsky SH, Glaser R. Norepinephrine upregulates VEGF, IL-8, and IL-6 expression in human melanoma tumor cell lines: implications for stress-related enhancement of tumor progression. Brain Behav Immun 2009;23(2):267–275. [PubMed: 18996182]

[92]. Yang EV, Sood AK, Chen M, Li Y, Eubank TD, Marsh CB, Jewell S, Flavahan NA, Morrison C, Yeh PE, Lemeshow S, Glaser R. Norepinephrine up-regulates the expression of vascular endothelial growth factor, matrix metalloproteinase (MMP)-2, and MMP-9 in nasopharyngeal carcinoma tumor cells. Cancer Res 2006;66(21):10357–10364. [PubMed: 17079456]

[93]. Ye Y, Bernabe DG, Salvo E, Viet CT, Ono K, Dolan JC, Janal M, Aouizerat BE, Miaskowski C, Schmidt BL. Alterations in opioid inhibition cause widespread nociception but do not affect anxiety-like behavior in oral cancer mice. Neuroscience 2017;363:50–61. [PubMed: 28673713]

[94]. Ye Y, Dang D, Zhang J, Viet CT, Lam DK, Dolan JC, Gibbs JL, Schmidt BL. Nerve growth factor links oral cancer progression, pain, and cachexia. Mol Cancer Ther 2011;10(9):1667–1676. [PubMed: 21750223]

[95]. Ye Y, Scheff NN, Bernabe D, Salvo E, Ono K, Liu C, Veeramachaneni R, Viet CT, Viet DT, Dolan JC, Schmidt BL. Anti-cancer and analgesic effects of resolvin D2 in oral squamous cell carcinoma. Neuropharmacology 2018;139:182–193. [PubMed: 30009833]

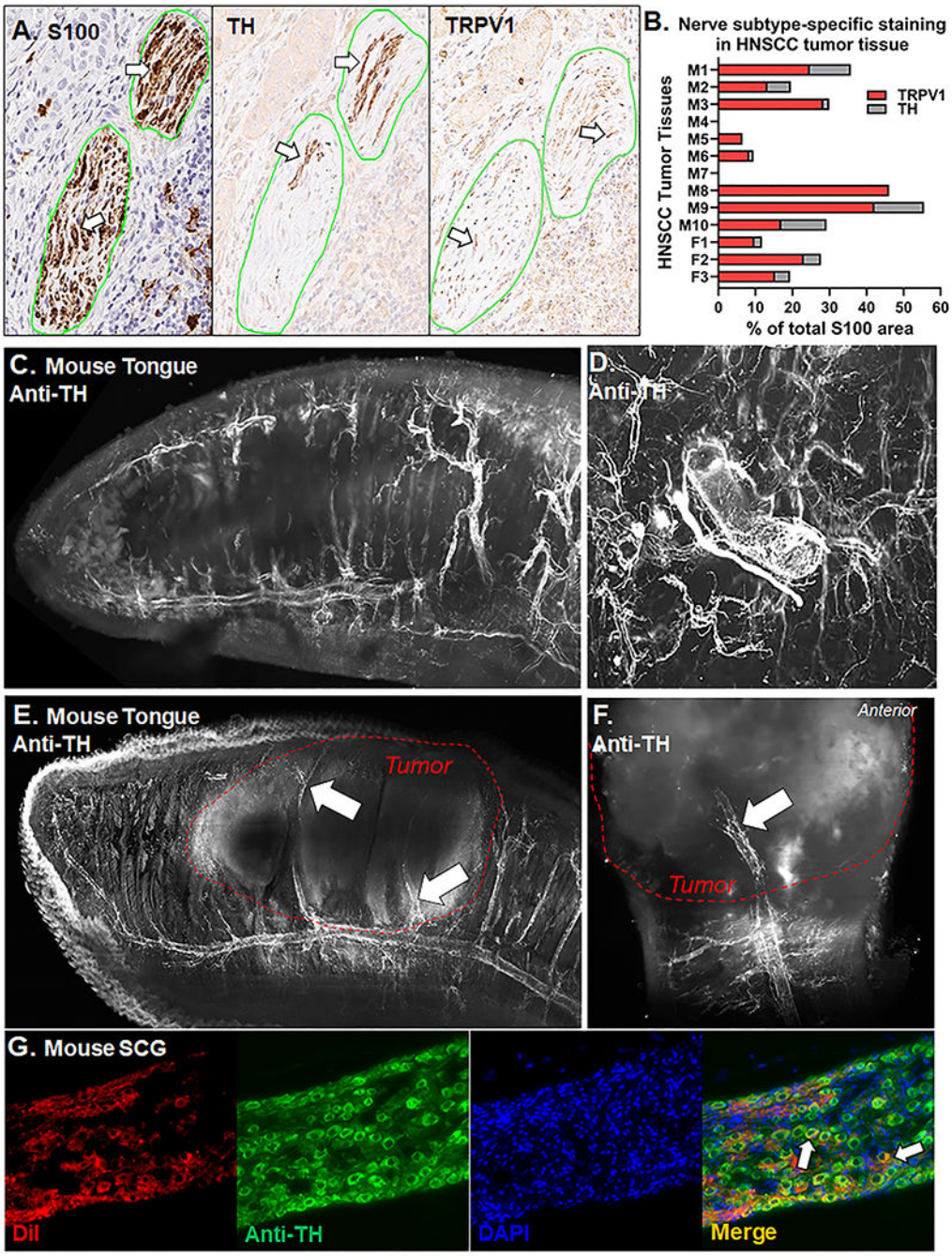

Figure 1: Anti-tyrosine hydroxylase (TH) immunoreactivity (IR) in tissue from HNSCC patients and oral cancer mouse models.

A) Representative images of HNSCC tumor serial tumor sections (5μm) stained with either S100 (left), TH (middle), or TRPV1 (right). Nerve bundles are outline in green and positive stain is indicated by white arrows. Image magnification = 20x. **B)** Quantification of the percent of total TRPV1-IR (red bars) and TH-IR (gray bars) nerve area relative to total S100-IR nerve area across tumor tissue sections from 13 HNSCC patients with PNI denoted pathology reported by an oral and maxillofacial pathologist. Patient sex is demarcated

with an M or F on the y axis. Patient demographics are located in Suppl Table 1. **C)** Representative image of TH-IR in a bisected optically cleared tongue from a naïve nude athymic female mice (n=2, 2.5x magnification). **D)** TH-IR innervation encircling an artery within the tongue muscle. Two different angles (side view 2.5x magnification, **E**; top view 3.63x, **F**) of TH-IR in bisected optically cleared tongues from a nude athymic mice bearing an HSC-3 tumor at post-inoculation day 28 (n=4). Tumor boundary is outlined in a red hashed line. TH-IR innervation within the HSC-3 tumor is indicated by white arrows. **G)** Representative images of retrograde labeling (DiI, red) and anti-TH immunoreactivity (green) in the SCG from a naïve adult female C57Bl/6 mice (n=3) 10 days after DiI injection into the tongue. Overlap of enodogenous DiI labeling and TH-IR (Merge, yellow) are indicated by white arrows.

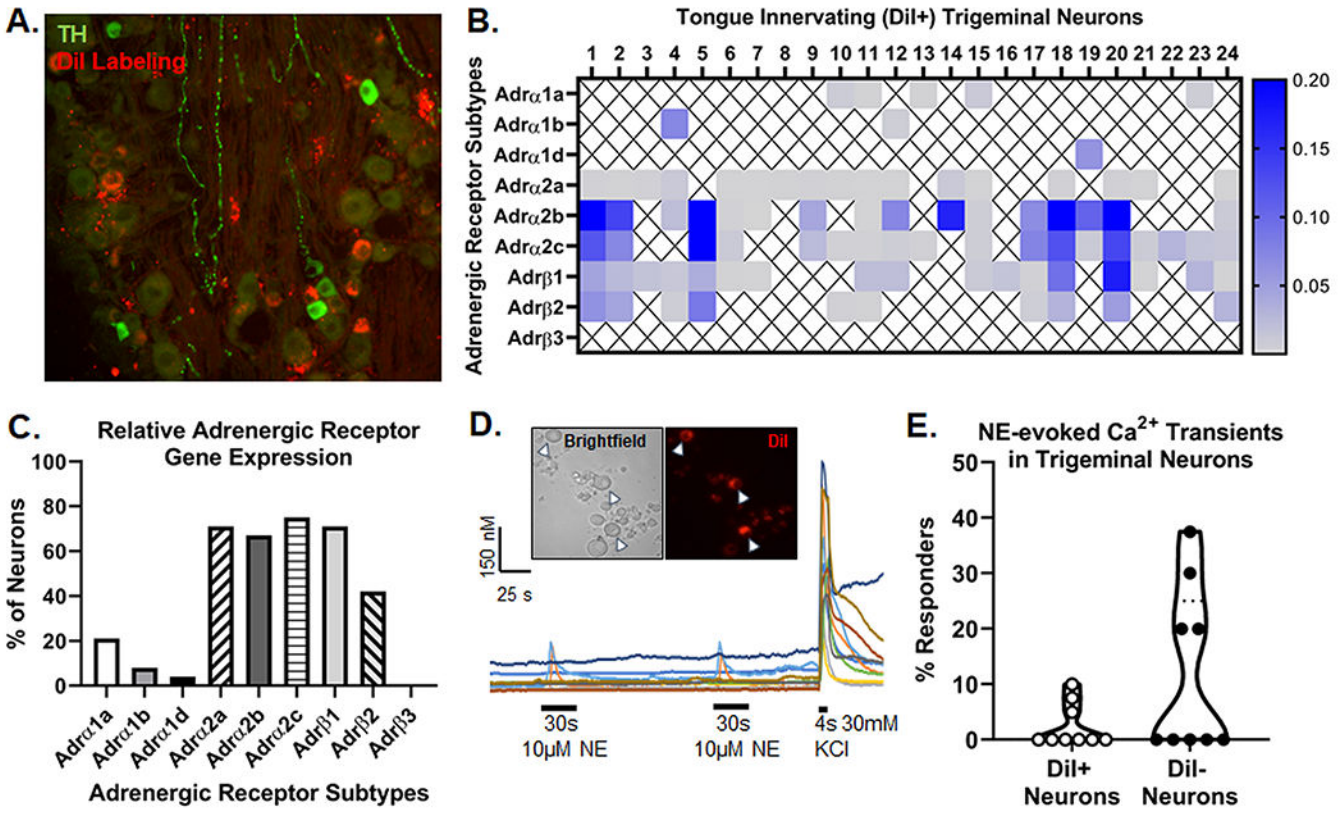

Figure 2. Anti-tyrosine hydroxylase (TH) staining and adrenergic signaling in tongue trigeminal ganglia neurons (TGN).

A) Representative images of retrograde labeling (red) and anti-TH immunoreactivity (green) in the mandibular branch of the TG from an adult female C57Bl/6 mouse 10 days after DiI injection into the tongue. **B)** Adrenergic receptor subtype gene expression from retrogradely labeled (DiI+) tongue-innervating TG neurons from 2 female C57Bl/6 mice that were manually picked to perform single-cell PCR. Gene expression was calculated for relative mRNA expression for each cell for each gene. *Gapdh* was used as an internal control. Data are presented as heatmap for each gene for each cell. An X indicated that expression was below the level of detection (CT<38) for that cell. **C)** Number of DiI+ neurons expressing each gene were counted and presented as percentage of neurons expressing the target gene. **D)** Representative Ca^{2+} imaging traces demonstrate the evoked Ca^{2+} transient in response to 10μM NE applied for 30 sections to a (*Inset*) mixed field of dissociated TGN containing both retrograde labeled (DiI+, arrow heads) and non-labeled (DiI−) cells. KCl-evoked depolarization (30mM, 4s) was used to establish cell viability in the field. **E)** Quantitative analysis of the percent of NE-responsive DiI− and DiI+ neurons across 9 mice (5 C57Bl/6, 4 nude). A neuron was considered responsive if NE evoked a Ca^{2+} transient ≥20% of baseline Ca^{2+} concentration. At least 15 neurons were assessed per mouse and the percent of responsive neurons per mouse are depicted to representent biological variance.

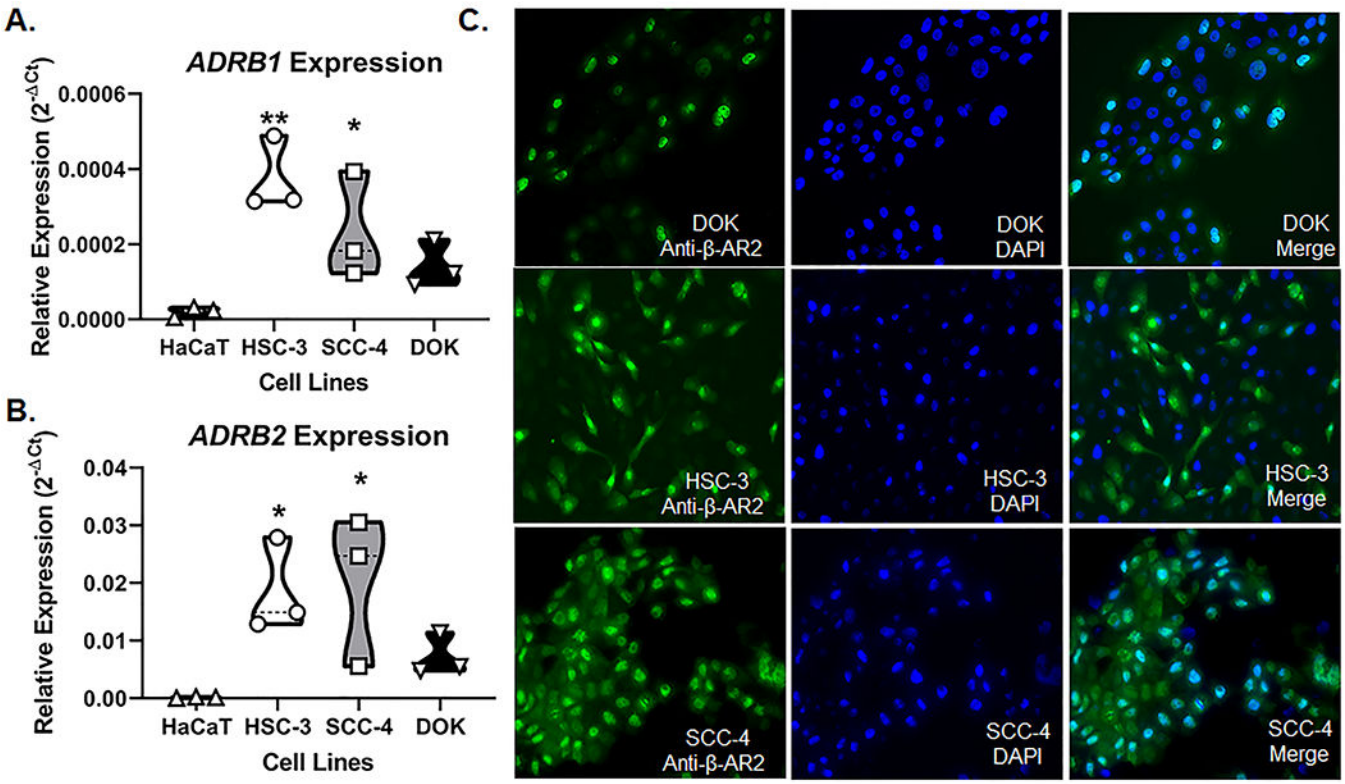

Figure 3. β-adrenergic receptor (β-AR) expression in oral cancer cells.

RT-qPCR was used to quantify relative *ADRB1* **(A)** and *ADRB2* **(B)** gene expression in oral cancer (HSC-3, SCC-4) and dysplastic (DOK) cells compared to non-tumorigenic skin keratinocytes (HaCaT). Data is presented as the relative gene expression ($2^{-\Delta CT}$) normalized to *ACTB* and represent three different cell passage determinations of gene expression. *p<0.05, **p<0.01. **C)** Representative images of β-AR2-IR (green) in DOK, HSC-3, and SCC-4 cell lines. DAPI (blue) was used to label cell nuclei.

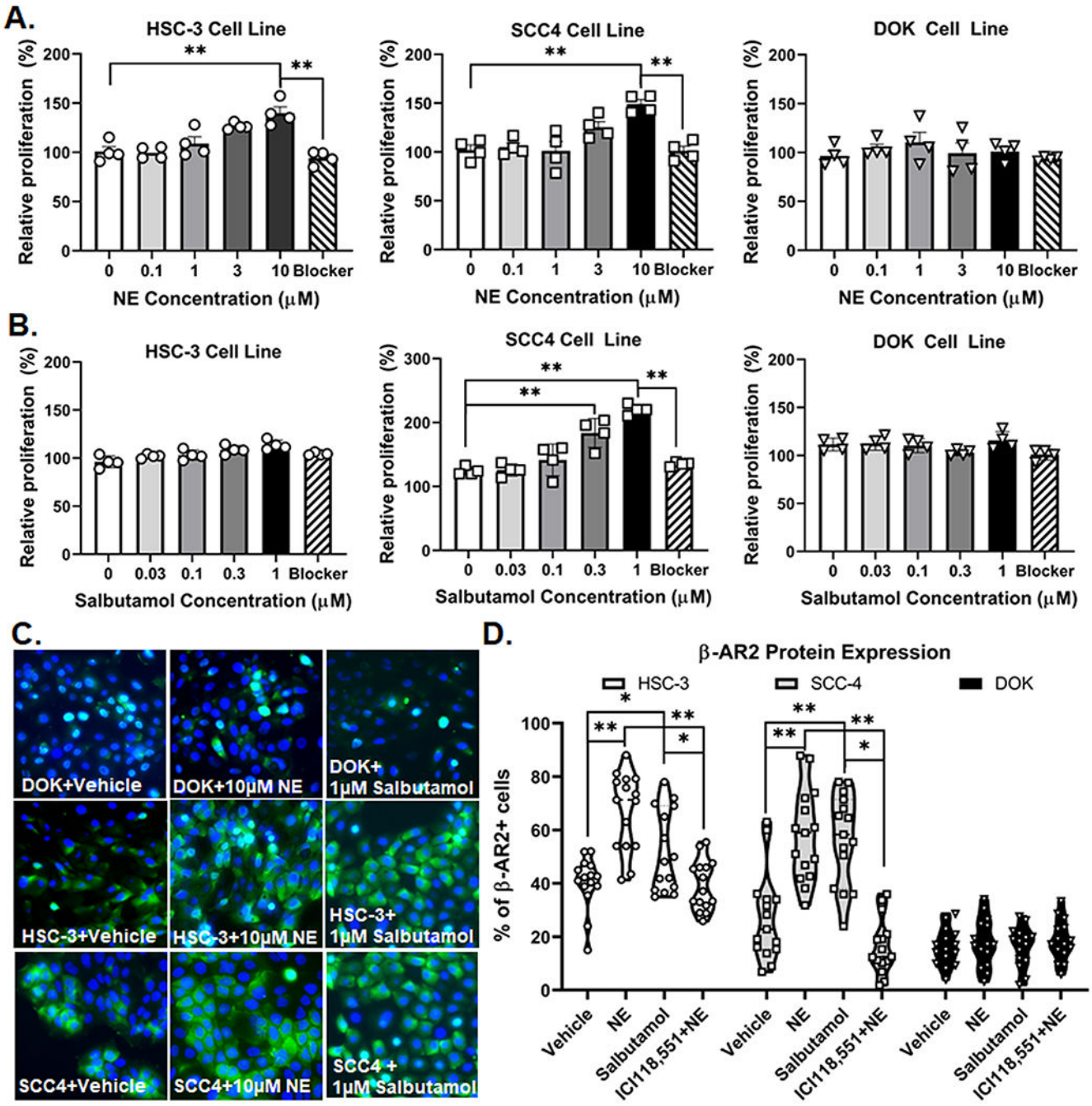

Figure 4. Norepinephrine (NE) increase proliferation and β-adrenergic receptor 2 (β-AR2) expression in oral cancer cells.

A) NE and **B)** Salbutamol MTS cell proliferation assays were used to determine change in cell growth after NE stimulation. The optical densities of non-stimulated vehicle-treated cells were set as 100%, and the proliferation of treated cells was determined relative to non-stimulated cells. Blocker indicates co-treatment with (A) 10μM NE and 10μM propranolol or (B) 1μM Salbutamol and 10μM propranolol. Data represent the mean (±SEM) of three different cell passage determinations of cell proliferation. **p<0.01. **C)** Representative

images of β-AR2-IR (green) in DOK, HSC-3, and SCC-4 cell lines treated with vehicle (0.05% HCl, 0.02% water), 10μM NE, and 1μM Salbutamol. Competitve β2 agonist, 1μM ICI 118,551, was used to inhibit effects of NE. DAPI (blue) was used to label cell nuclei. **D)** Quantitative analysis of cells with distinct DAPI labeled nuclei and β-AR2-IR across treatments groups. *$p<0.05$ **$p<0.01$

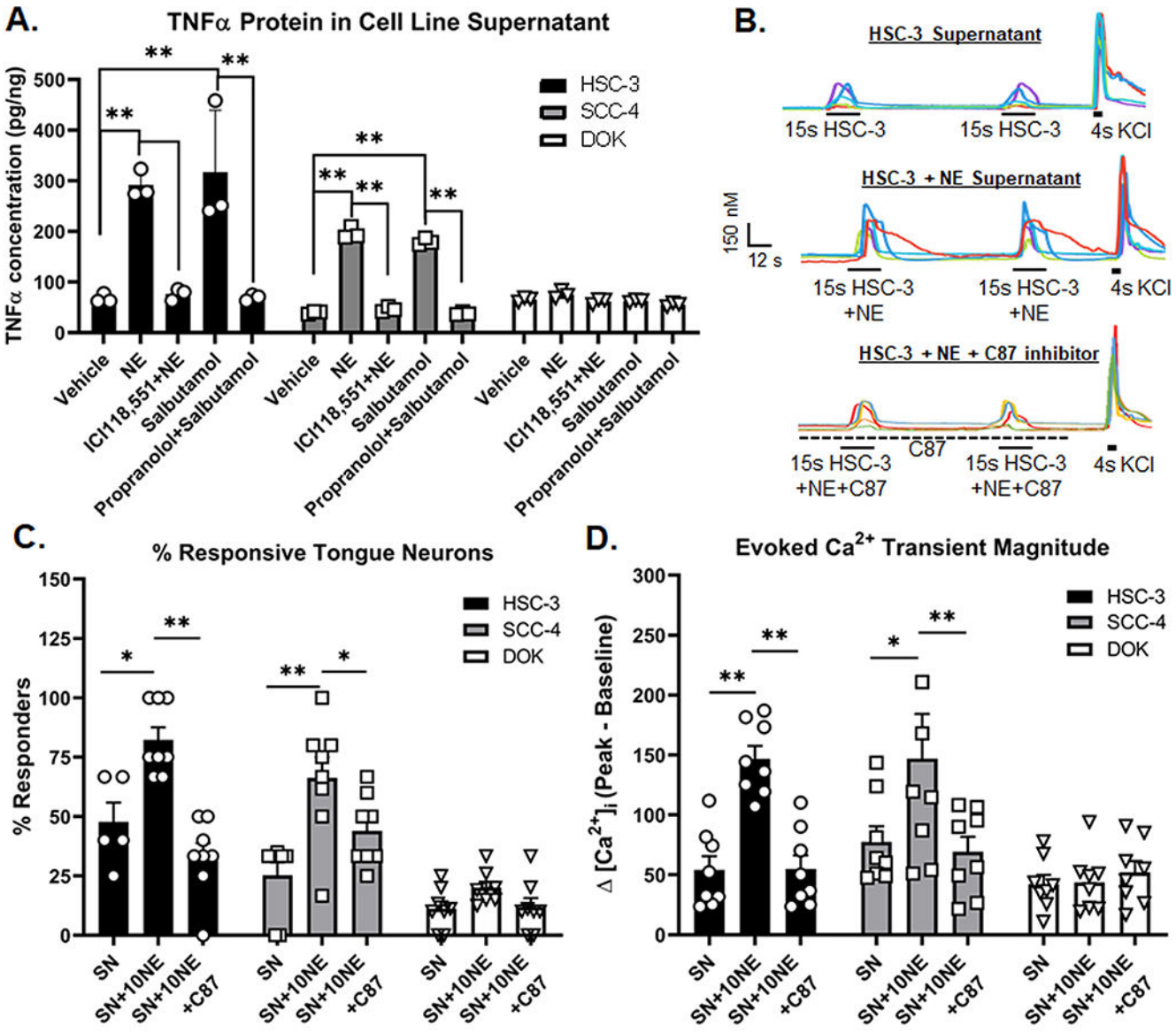

Figure 5. Norepinephrine (NE) stimulation increases cancer cell TNFα secretion and trigeminal ganglia neuron (TGN) activation.

A) Supernatant (SN) from oral cancer (HSC-3, SCC-4) and dysplasia (DOK) were collected 48 h after stimulation with vehicle (0.05% HCl, 0.05% EtOH, 0.02% water), 10μM NE, 1μM ICI118,551 and 10μM NE, 1μM Salbutamol, and 10μM propranolol and 1μM Salbutamol. Blockers were added 1 hour prior to the addition of agonists. Data represent the mean (±SEM) of three different cell passage determinations of TNFα concentration. **p<0.01. **B)** Example traces of HSC-3 supernatant-evoked (top), 10μM NE-stimulated HSC3 supernatant-evoked (middle) and 10μM NE-stimulated HSC-3 SN in the presence of TNF inhibitor, C87, evoked (bottom) Ca^{2+} transients. KCl-evoked depolarization (30mM, 4s) was used to establish cell viability. Quantitative analysis was performed to generate **(C)** percent responders and **(D)** magnitude of the evoked Ca^{2+} transient in response to stimulation from SN (n=8 mice), 10μM NE-stimulated supernatant-evoked (SN+NE, n=8

mice) and 10μM NE-stimulated SN in the presence of C87 (SN+10NE+C87, n=8 mice). Transient magnitude was calculated as peak minus baseline Ca^{2+} concentration. There was no C87 vehicle control (0.02% DMSO) included in the supernatant samples. *p<0.05, **p<0.01

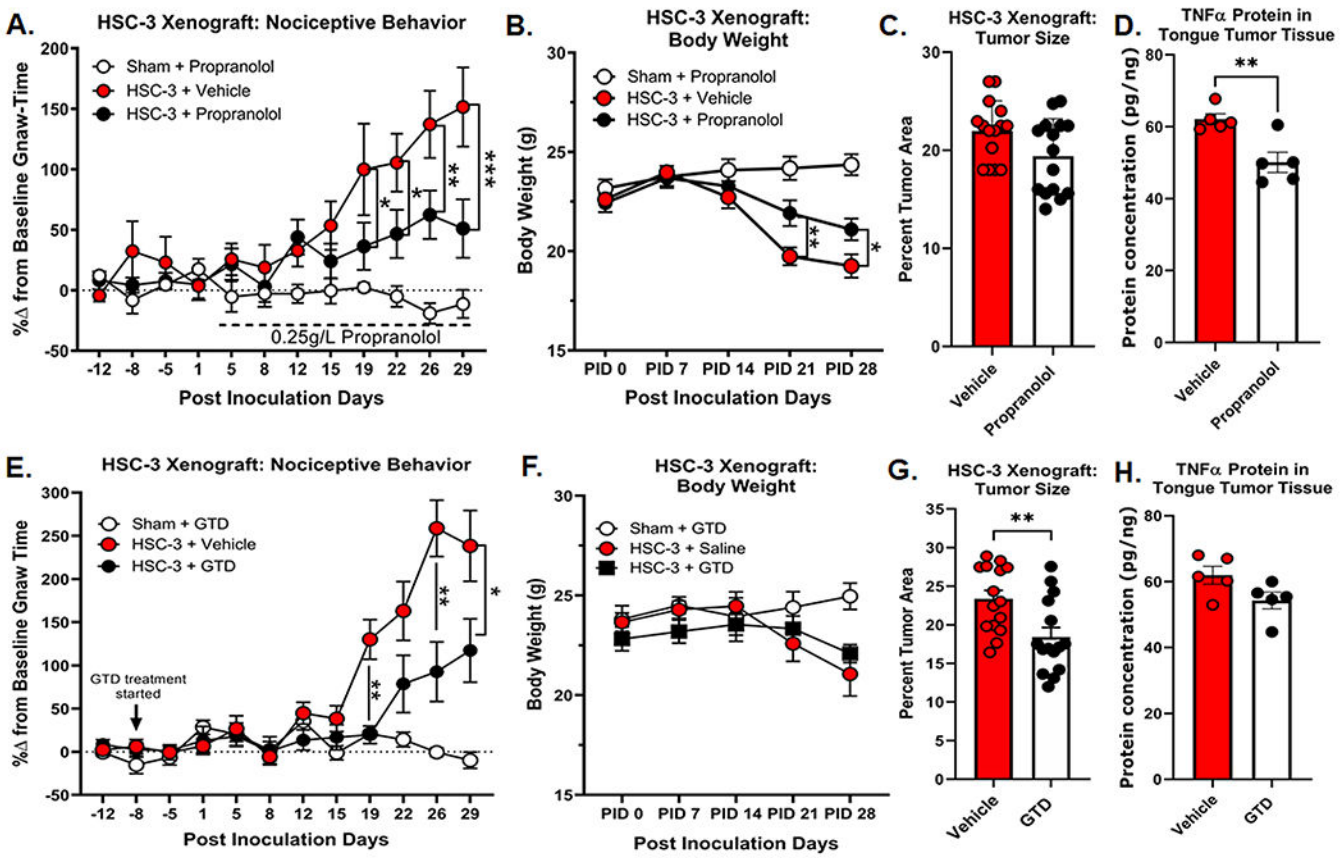

Figure 6. Disruption of norepinephrine (NE) signaling attenuates oral cancer-induced nociceptive behavior and tumorigenesis.

Orofacial nociceptive behavior was measured in adult nude female sham and HSC-3 tumor bearing mice. Two weeks of baseline orofacial nociceptive behavior was acquired prior to inoculation. Mice were inoculated at PID 0. **A)** Quantitative analysis of the percent change in baseline gnaw-time in sham mice receiving β-adrenergic receptor (β-AR) antagonist propranolol (0.25g/L n=10, open circles), or HSC-3 tumor-bearing female mice receiving vehicle (saline, n=15, red circles) or 0.25g/L propranolol (n=15, black circles). Propranolol treatment began on PID 3 as indicated by the dotted line. *p<0.05, **p<0.01, ***p<0.001. **B)** HSC-3 xenograft-induced weight loss was measured weekly across all groups (n=15/group) and compared to sham-treated mice. **C)** HSC-3 xenograft tumor size and TNFα protein concentration in the tumor **(D)** were measured at post-innoculation day (PID) 28. Tumor area was calculated relative to total tongue area after treatment with either vehicle or propranolol (n=15/group). TNFα protein was measured by ELISA (n=5/group) and normalized to total protein isolated in the tongue tumor tissue. Student t test **p<0.01. **E)** Quantitative analysis of the percent change in baseline gnaw-time in sham mice receiving NE reuptake inhibitor guanethidine (GTD; 0.5mg/mouse, n=10, open circles), or HSC-3 tumor-bearing female mice receiving vehicle (saline, n=15, red circles) or GTD (n=15, black circles). GTD treatment began on PID −8 as indicated by the black arrow. *p<0.05, **p<0.01. **F)** HSC-3 xenograft-induced weight loss was measured weekly across all groups and compared to sham-treated mice. **G)** HSC-3 xenograft tumor size and TNFα protein

concentration in the tumor **(H)** were measured at post-innoculation day (PID) 28. Tumor area was calculated relative to total tongue area after treatment with either vehicle or GTD (n=15/group). TNFα protein was measured by ELISA (n=5/group) and normalized to total protein isolated in the tongue tumor tissue. Student t test **p<0.01.

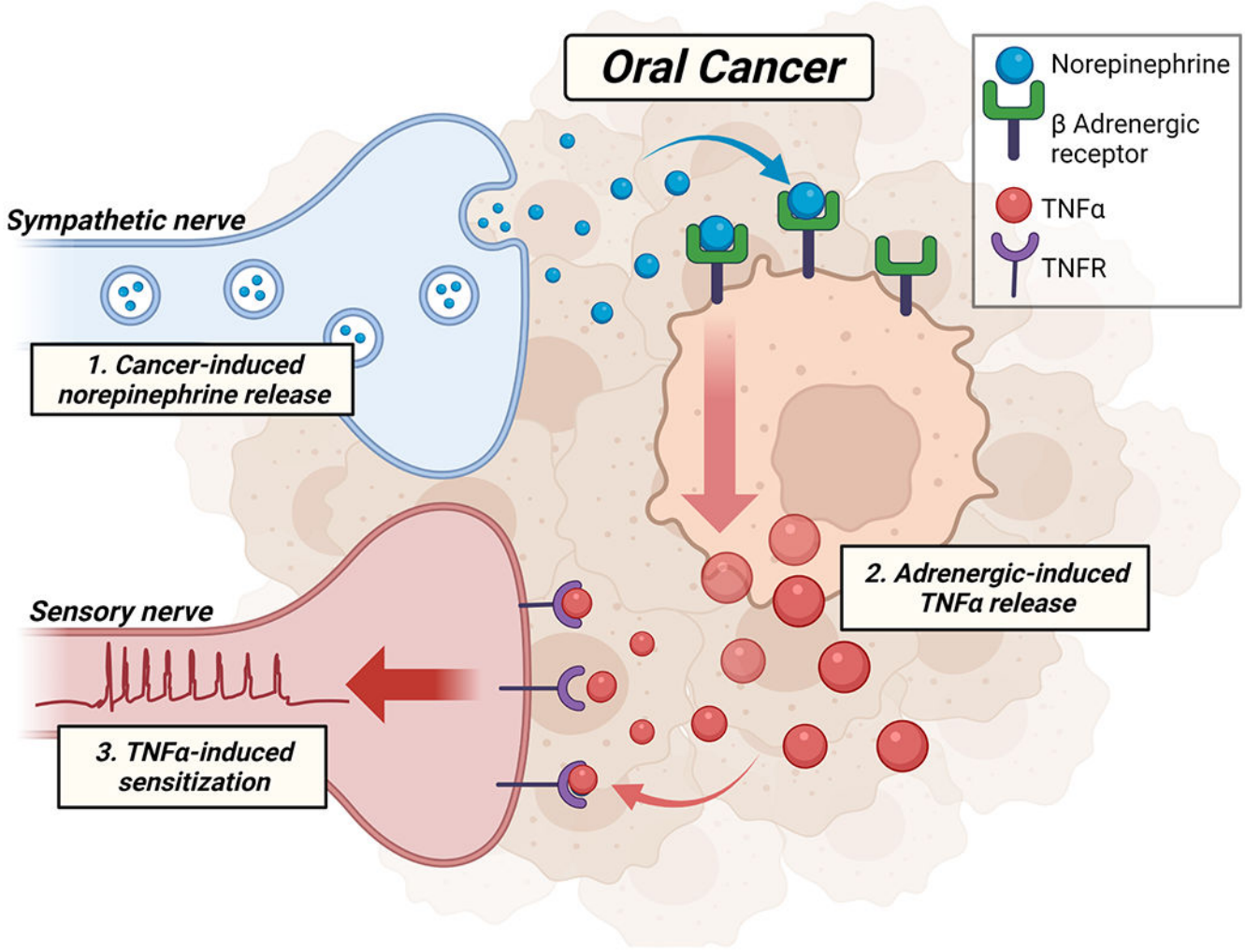

Figure 7. Schmatic representation of sympathetic modulation of oral cancer pain.

We hypothesize that in the oral cancer microenvironment (1) sympathetic nerves release norepinephrine which binds to β-adrenergic receptors expressed on oral cancer cells. (2) Tumor necrosis factor α (TNFα) is subsequently secreted from tumor cells in response to adrenergic activation and binds to TNF receptors expressed on tumor innervating sensory nerves resulting in (3) sensory nerve sensitization and pain signaling.

Table 1:

Adrenergic expression in naïve mouse trigeminal ganglia

Adrenergic Receptor Subtype	ΔCT (relative to *Gapdh*)	
	C57BI/6	Athymic
Adra1a	10.40 ± 0.36	9.96 ± 0.26
Adra1b	11.67 ± 0.31	10.53 ± 0.77
Adra1d	10.55 ± 0.29	9.98 ± 0.29
Adra1a	10.87 ± 0.73	10.42 ± 0.34
Adra1b	11.47 ± 0.35	10.41 ± 0.37
Adra1c	5.89 ± 0.22	6.63 ± 0.26
Adrb1	10.12 ± 0.27	9.90 ± 0.70
Adrb2	9.17 ± 0.51	9.00 ± 1.21
Adrb3	Not detected	Not detected

Adra, adrenergic receptor alpha; Adrb, adrenergic receptor beta. The cycle threshold (CT) for each gene was normalized to the housekeeping gene, *Gapdh*. “Not detected” indicates the expression was below the level of detection for that gene (i.e. CT<38). Values are displayed as mean ± s.e.m. N-values are provided in parentheses in genotype column and represent number of male and female animals.